MASTERARBEIT | MASTER'S THESIS

Titel | Title

Investigating gene expression under different dietetic conditions in murine skeletal muscle and brown adipose tissue

verfasst von | submitted by

Elise Lenz BSc

angestrebter akademischer Grad | in partial fulfilment of the requirements for the degree of

Master of Science (MSc)

Wien | Vienna, 2025

Studienkennzahl lt. Studienblatt | Degree programme code as it appears on the student record sheet:	UA 066 838
Studienrichtung lt. Studienblatt | Degree programme as it appears on the student record sheet:	Masterstudium Ernährungswissenschaften
Betreut von | Supervisor:	Univ.-Prof. Dr. Jürgen König
Mitbetreut von | Co-Supervisor:	Dr. Felix Sternberg B.rer.nat. MSc

Table of contents

1. Abstract

Fatty acids (FA) play an essential role in human nutrition, serving both as energy substrates and structural components of cells. Ketogenic diets (KD), in which fats constitute the primary source of caloric intake, have been used for 100 years to treat drug-resistant epilepsy in children. More recently, KDs have received renewed attention as a potential therapy for neurodegenerative diseases, as a dietary intervention for weight loss, and for a range of other clinical applications. Understanding the biological and molecular mechanisms behind lipid metabolism, along with the physiological benefits and downsides of a high dietary fat consumption is therefore crucial for understanding the possible effects of KDs on human health and disease.

In previous studies by Sternberg et al. (2025, unpublished data), gene expression related to FA metabolism was analyzed in mice fed KDs differing in FA profiles focusing on skeletal muscle (SkM), brown adipose tissue (BAT), heart, liver and brain tissues. The results revealed that mice receiving a KD enriched with medium-chain triglycerides (LCT/MCT), exhibited a distinct gene expression profile reflecting enhanced FA metabolism, compared with those fed either a long-chain triglyceride KD (LCT) or a standard diet (SD). Building on these findings, the present study further investigated gene expression profiles related to lipid metabolism and mitochondrial function in BAT and SkM using quantitative real-time polymerase chain reaction, aiming to provide deeper insights into the molecular pathways through which different types of dietary fat influence lipid utilization and mitochondrial transcriptional states.

Consistent with previous observations, the LCT/MCT diet induced significant transcriptional adaptations in both BAT and SkM. While both tissues likely increased fatty acid oxidation, BAT appeared to shift its substrate preference by inhibiting fatty acid synthesis, whereas SkM exhibited signs of reduced long-chain fatty acid oxidation. Furthermore, BAT showed transcriptional changes indicative of increased mitochondrial fission and elevated oxidative stress.

2. Ketogenic diets

The ketogenic diet (KD) is characterized by a high fat intake, minimal carbohydrates and moderate amounts of protein. A classical KD typically provides approximately 1 g of protein per kg body weight and 10-15 g of carbohydrates per day, with the remaining caloric intake derived from fat. (Roehl & Sewak, 2017) Its primary goal is to induce a metabolic state known as ketosis, in which the body shifts from glucose to ketone bodies (KB), namely acetone, acetoacetate and β-hydroxybutyrate (β-OHB), as its main energy source. When carbohydrate intake is restricted, as during fasting or adherence to a KD, hepatic KB production increases. (St-Pierre et al., 2019)

The KD was originally developed as a fasting-mimicking therapy for epilepsy, following historical observations that fasting reduced seizure frequency. In the 1920s, the KD was introduced as a sustainable alternative to fasting, capable of inducing similar metabolic effects without causing malnutrition. With the discovery of the antiepileptic drug phenytoin in 1938, and as more medications became available, the clinical use of KDs declined. Nevertheless, due to the anticonvulsant properties of KBs, KDs are a well-established and commonly applied treatment for drug-resistant epilepsy. Since traditional KDs can be difficult to maintain, adapted versions such as KDs enriched with medium-chain triglycerides (MCT) have been explored in the 1980s as less restrictive alternatives to the traditional KD. Subsequently, the Modified Atkins Diet (MAD) and the Low Glycemic Index Treatment (LGIT) have been developed to improve palatability and make long-term adherence easier. (Borowicz-Reutt et al., 2024; Nimbkar et al., 2022; Roehl & Sewak, 2017; Wheless, 2008)

Beyond epilepsy, KDs have gained attention as potential therapeutic interventions for a wide range of applications. The KD and KBs exert neuroprotective effects by enhancing mitochondrial function and reducing both oxidative stress and neuroinflammation. Consequently, they are being investigated as a potential therapy for various neurological conditions, including neurodegenerative diseases, depression and migraines. (Haslam et al., 2021; Jang et al., 2023; Pietrzak et al., 2022; Włodarek, 2019) Moreover, KDs are being explored for effects beyond the nervous system, with studies investigating potential benefits in cardiovascular disease

(Dyńka et al., 2023), metabolic syndrome and obesity (Wang et al., 2018), and improving lipid profiles and body weight. (Choy & Louie, 2023; Zhou et al., 2022) Additional areas of research include adjunctive cancer therapies (Talib et al., 2021), autism spectrum disorders (Öztürk et al., 2024), and gastrointestinal inflammation. (Gregor et al., 2022) Furthermore, KDs have recently gained popularity because of their supposedly positive effects on weight loss.

At the molecular level, KDs and KBs influence a wide range of cellular processes, including the reduction of apoptosis, increase of autophagic flux, regulation of gene expression and epigenetic and post-translational modifications of histones and other proteins. In addition, they affect the modulation of neurotransmitter systems and the gut microbiome. (Jang et al., 2023)

Although KDs have been shown to reduce body mass, triglycerides (TG), HbA1c and blood pressure in the short-term, their long-term effects remain unclear. (Popiolek-Kalisz, 2024) Evidence regarding the impact of KDs and MCTs/medium-chain fatty acids (MCFA) on TG and cholesterol levels over extended periods of time is insufficient. Consequently, the long-term impact of KDs on cardiovascular disease risk factors should be carefully monitored during adherence to the diet. (Corsello et al., 2023; Huang et al., 2021)

Despite their therapeutic promise, emerging evidence also indicates possible adverse effects. The classical KD has been associated with complications including gastrointestinal issues, dehydration, kidney stone formation and liver dysfunction. Additionally, the classic KD may lead to growth retardation in children and impaired bone mineralization in adolescents. But it remains to be determined whether this effect is due to the KD itself, or the underlying pathology and administered medication, as the primary target group for KDs are children with epilepsy. The MAD, LGIT and MCT-KD have been reported to cause fewer side effects and are generally better tolerated and palatable than the classic KD. Individuals with disorders affecting lipid or pyruvate metabolism should avoid KDs, as such conditions may lead to life-threatening complications (Borowicz-Reutt et al., 2024; Ferraris et al., 2019; Merlotti et al., 2021)

In mice, KDs have been reported to exert pro-inflammatory effects in the liver, (Asrih et al., 2015) exacerbate colitis (Li et al., 2021) and induce cardiac fibrosis. (Sternberg et al., 2023) Similarly in rats, a prolonged KD and exogenous β-OHB administration led to cardiac fibrosis and reduced mitochondrial biogenesis. (Xu et al., 2021) Furthermore, a KD may increase cellular senescence through p53 accumulation and induction of p21. (S.-J. Wei et al., 2024)

Adhering to a KD is a complex and demanding process. The classical KD typically follows a strict 4:1 or 3:1 ratio of grams of fat to combined grams of protein and carbohydrates, requiring precise calculation and weighing of macronutrient intake, as even a slight increase in carbohydrate consumption can disrupt ketosis. To ensure safety and effectiveness, the diet should be implemented under medical and nutritional supervision with regular monitoring of nutritional status, especially in pediatric patients. Since patients following a KD are often at risk of inadequate micronutrient levels, appropriate supplementation is necessary to prevent malnutrition. Furthermore, the KD is often considered unpalatable and can be difficult to maintain over extended periods, posing additional challenges to adherence and compliance. (Corsello et al., 2023; Roehl & Sewak, 2017)

Even though KDs have been in use for a long time, their long term metabolic effects are still not fully understood, emphasizing the need for further studies. (Corsello et al., 2023)

3. Intermittent fasting and calorie restriction

Because KDs mimic the metabolic state of traditional fasting, it is speculated that the metabolic effects of intermittent fasting may resemble those of a KD, particularly when supplemented with MCTs. Caloric restriction on the other hand, is a well-established intervention to promote longevity through the modulation of AMP-activated protein kinase (AMPK) and insulin signaling pathways.

Both intermittent fasting and caloric restriction are dietary interventions that limit food intake without necessarily altering the nutritional composition of the diet. While intermittent fasting restricts the time window during which food is consumed, the overall caloric intake is reduced with caloric restriction. Importantly, both

approaches are designed to induce benefits while avoiding malnutrition. Because of the lower palatability of KDs and the restricted eating window of intermittent fasting, a caloric restriction group is useful for isolating the effect of unintentional caloric restriction in the other groups.

Energy restriction leads to reduced adenosine triphosphate (ATP), increased adenosine monophosphate (AMP) levels and subsequent activation of AMPK, a key metabolic sensor of energy levels. Activated AMPK promotes catabolic pathways that generate ATP, while concurrently inhibiting energy-consuming anabolic processes. Consequently suppressing fatty acid synthesis (FAS) by inhibiting acetyl-CoA carboxylases (ACC) and downregulating fatty acid synthase (FASN), limiting *de novo* FAS of long-chain fatty acids (LCFA). (Lage et al., 2008)

Activated AMPK promotes mitochondrial biogenesis by stimulating the peroxisome proliferator-activated receptor gamma coactivator 1-alpha (PGC-1α). This results in a preferential use of fatty acids (FA) via β-oxidation over glucose as the primary energy source in skeletal muscle (SkM). PGC-1α stimulates the oxidation of FAs by activating the nuclear receptor peroxisome proliferator-activated receptor gamma (PPARγ) and reduces the production of reactive oxygen species (ROS). Additionally, AMPK activation upregulates the transcription and activity of the tumor suppressor p53 (p53), further supporting cellular stress responses and mitochondrial function. (Karagöz & Gülçin Sağdıçoğlu Celep, 2023)

The KD, MCTs, caloric restriction and intermittent fasting are all believed to induce this pathway, although their effects are tissue- and context-dependent. Similar to MCTs and KBs, a caloric restriction diet may induce AMPK activation, subsequently activating PGC-1α and mitochondrial biogenesis pathways, and ultimately contribute to life-prolonging effects. (Karagöz & Gülçin Sağdıçoğlu Celep, 2023; Kolb et al., 2021; Nishida et al., 2024) Comparable effects have also been observed with intermittent fasting, although its impact is dependent on the duration and type of fasting regimen as well as the organism studied. (Longo et al., 2021) Additionally, energy restriction has been shown to induce the browning of WAT, thereby enhancing thermogenic activity. (Karagöz & Gülçin Sağdıçoğlu Celep, 2023)

4. Mitochondrial dynamics

Mitochondria are double-membraned organelles composed of an inner mitochondrial membrane (IMM) and an outer mitochondrial membrane (OMM). They host key metabolic processes essential for energy production, including the tricarboxylic acid cycle, β-oxidation, and oxidative phosphorylation (OXPHOS). To meet the energy demands of the cell, mitochondria continuously adapt and remodel their morphology by undergoing fission and fusion. This dynamic behavior is fundamental for cell division and crucial for maintaining mitochondrial health. (Ngo et al., 2023; Tábara et al., 2024) Due to tissue-specific metabolic demands, mitochondrial morphology is finely adapted to the specialized functions of each cell type. (Wai & Langer, 2016)

Mitochondrial fusion is mainly regulated by mitofusin-1 (MFN1), mitofusin-2 (MFN2) and dynamin-like GTPase optic atrophy 1 (OPA1). While fission is mainly mediated by dynamin-1-like protein (DRP1) and the OMM proteins mitochondrial fission factor (MFF) for midzone fission and mitochondrial fission 1 protein (FIS1) for peripheral fission. (Kleele et al., 2021; Tábara et al., 2024) Fusion refers to the merging of mitochondria, while fission describes their division. Because both processes occur simultaneously, assessing the net morphological changes can be complicated. The term “mitochondrial fragmentation” refers to a shift towards smaller and more numerous mitochondria, which may result from increased fission, reduced fusion or a combination of both. (Ngo et al., 2023) Conversely, “mitochondrial elongation” describes the opposite phenomenon, characterized by longer, more interconnected mitochondrial networks. (Tábara et al., 2024)

Mitochondrial fission is known to serve multiple roles, including mitochondrial biogenesis, the repair of damaged mitochondria and adaptation to environmental factors such as available carbon sources. However, how the cell determines the specific purpose of each fission event remains unclear. Kleele et al. (2021) recently discovered that mitochondrial fission occurs in two ways that are functionally and mechanistically different. These can be categorized by the location of the fission event in peripheral and midzone fission. Peripheral fission acts as a quality control mechanism, targeting damaged mitochondrial segments for removal via

mitophagy, while midzone fission is primarily associated with mitochondrial proliferation. (Kleele et al., 2021)

Mitochondrial fusion increases the organelles cross-sectional area, optimizing OXPHOS capacity while decreasing glycolysis. In contrast, mitochondrial fission exerts the opposite effect, decreasing OXPHOS and promoting glycolysis. (Noone et al., 2022) Furthermore, fission is associated with high stress conditions such as mitochondrial dysfunction. It occurs under glycolytic conditions and as a response to the activation of AMPK and mTOR (mammalian target of rapamycin) pathways. (Tábara et al., 2024) In addition, fission is necessary as a response to excess fat and general nutrient overload to increase carnitine palmitoyltransferase 1 (CPT1)-mediated fatty acid oxidation (FAO). (Ngo et al., 2023)

Fusion can be induced by conditions such as energy deprivation, and is thought to be a protective mechanism with the purpose of maintaining mitochondrial function. By enhancing OXPHOS, the elongation promotes cell survival and protects mitochondria from degradation. (Liesa & Shirihai, 2013; Tábara et al., 2024) However, increased mitochondrial fragmentation leads to a higher lipid oxidation capacity due to the reduced sensitivity of CPT1 to malonyl-CoA and a higher preference for lipids as an energy source in human cells. (Ngo et al., 2023) Notably, the interplay between OXPHOS activity and mitochondrial dynamics is highly complex and context-dependent.

Dysregulation of mitochondrial morphology can contribute to cellular senescence through the influence of p53 on DRP1 activity. (Kim et al., 2020) Sustained extensive elongation is associated with senescence-associated phenotypic changes. (Lee et al., 2007) Moreover, the impairment of fusion, caused by deficiencies of MFN1, MFN2 or OPA1, results in reduced mtDNA and exacerbates mitochondrial dysfunction. (Zanfardino et al., 2025)

Both brown adipose tissue (BAT) and SkM are rich in mitochondria, it is however challenging to compare mitochondrial activity between BAT and SkM, because the amount, activity and morphology of mitochondria varies between different tissues and cell types. Herbers et al. (2019) reported that mitochondrial DNA (mtDNA) content did not differ significantly, either per cell or normalized to tissue mass,

between BAT and SkM. Devine et al. (2025) found no consistent pattern of mitochondrial distribution across tissues. Some individuals may exhibit higher oxidative capacity in one tissue and lower in another, while others may show the opposite pattern.

5. Fatty acid metabolism

Fats play an essential role in the diet, serving as the main energy storage system in the body and function as signaling molecules and as components of cellular membranes. Therefore, optimal functioning of lipid metabolism is crucial for maintaining overall health.

The absorption, transport and oxidation of FAs differs depending on the chain length. LCFA require transport via the carnitine shuttle, a crucial mechanism for enabling their entry from the cytosol into the mitochondrial matrix, where β-oxidation occurs. In contrast, some MCFAs such as caprylic acid (C8:0) can permeate the mitochondrial membrane and are activated within the mitochondrial matrix. (Schönfeld & Wojtczak, 2016) After the activation of LCFAs to long-chain (LC)-fatty-acyl-CoA esters in the cytosol, they are conjugated by carnitine palmitoyltransferase 1 (CPT1) to L-carnitine to form acylcarnitines, enabling their transport into the mitochondria via the carnitine-acylcarnitine translocase (CACT), and are subsequently converted back into LC-fatty-acyl-CoAs by the carnitine palmitoyltransferase 2 (CPT2) in the mitochondrial matrix. (Figure 1) (Dambrova et al., 2022) Members of the acyl-CoA dehydrogenase family, namely very-long-chain acyl-CoA dehydrogenase (VLCAD), long-chain acyl-CoA dehydrogenase (LCAD), medium-chain acyl-CoA dehydrogenase (MCAD) and short-chain acyl-CoA dehydrogenase (SCAD) catalyze the first step of β-oxidation, each exhibiting substrate specificity based on FA chain length, as reflected in their names. (O'Leary et al., 2016) In mice, LCAD, along with the other acyl-CoA dehydrogenases, plays an important role in FAO, whereas in humans, LCAD appears to have a relatively minor contribution. (Martines et al., 2019)

Ketone bodies (KB) are predominantly synthesized in the liver from acetyl-CoA, which arises from FAO. They serve as alternative energy substrates, especially during glucose scarcity, and are transported to extrahepatic tissues such as the

brain and SkM. Although it has been proposed that astrocytes and other cell types are capable of extrahepatic ketogenesis, their contribution is likely small. (Puchalska & Crawford, 2017)

In addition to serving as an alternative energy substrate, KBs also function as signaling molecules. In conditions of limited glucose availability, such as during a ketogenic diet or starvation, the body experiences significant metabolic stress. β-OHB, the most abundant KB, serves as an indicator of this metabolic state, thus elevated KB levels may serve as an indicator of starvation. This mitochondrial stress induced through elevated ketolysis is characterized by higher ROS, nicotine adenine dinucleotide (NAD+) and AMP levels. These changes activate nuclear factor erythroid 2-related factor 2 (NRF2), sirtuin 1, sirtuin 3 and AMPK, thereby promoting anti-oxidative, anti-inflammatory pathways and mitochondrial function. Beyond these effects, β-OHB acts directly as a signaling molecule by influencing histone modifications and thereby regulating gene expression, notably through activation of the transcription factor forkhead box O3 (FOXO3a). Collectively, KB-induced stress responses trigger a cell-protective program that contributes to broader long-term benefits. (Kolb et al., 2021; Møller, 2020)

6. Medium chain triglycerides

Medium chain triglycerides represent a small but significant fraction of dietary fats. Due to their high ketogenic potential, they are of growing interest for maintaining health and managing disease. Many potential benefits are associated with MCT-intake, including improved cognitive function and beneficial effects on neurodegenerative diseases, potentially through the modulation of mitochondrial function and autophagy. (Dunn et al., 2023; Sun et al., 2024) Because of their rapid conversion into KBs, they can be partially substituted for long-chain triglycerides (LCT) in KDs, to enhance palatability. (Borowicz-Reutt et al., 2024)

It has been speculated, that MCFAs themselves, particularly caprylic acid (C8:0) and capric acid (C10:0), may exert neuroprotective effects that are independent of their ketogenic potential. They can regulate energy balance and mitochondrial function in neurons and enhance neuronal γ-aminobutyric acid synthesis. (Jensen et al., 2020; Lin et al., 2021)

MCTs are composed of MCFAs, typically defined as FAs with chain lengths of 6-12 carbon atoms. However, lauric acid (C12:0) is sometimes classified as either a medium- or long-chain FA due to its intermediate metabolic properties. In practice, the term “MCTs” often refers to only C8:0 and C10:0. Natural dietary sources include coconut oil, palm kernel oil and milk fat. Coconut oil is composed of about two-thirds MCTs, containing approximately 50% C12:0, 6% C8:0, 6% C10:0 and less than 1% caproic acid (C6:0) by weight. Palm kernel oil has a comparable overall MCT content, although its levels of C8:0 and C10:0 are roughly half those found in coconut oil. (Norgren et al., 2020; W. Wei et al., 2019) Milk fat is another natural source of MCTs, accounting for approximately 4–12% C6:0-C10:0 of the total FA content in various dairy products (Nimbkar et al., 2022), with butter containing around 10% MCFAs. (Pustjens et al., 2017) Notably, MCFAs in milk fat are incorporated into mixed TGs rather than occurring as pure MCT molecules. (Beccaria et al., 2014)

MCFAs are metabolized differently from LCFAs. Owing to their smaller size, they are transported directly to the liver via the portal vein, independent of digestion by bile salts or pancreatic lipase. In contrast, LCFAs are first packaged into micelles and transported through the lymphatic system. Once inside hepatocytes, MCFAs have been suggested to pass directly through the mitochondrial membranes without requiring the carnitine-shuttle. In the mitochondria, they are preferentially oxidized and more efficiently converted into KBs compared with LCFAs. (Cheng et al., 2024; Dunn et al., 2023; Nimbkar et al., 2022)

In humans, MCT intake results in higher β-OHB plasma levels compared to LCT consumption. (Sternberg et al., 2023) Among MCTs, the ketogenic potential of C8:0 is substantially greater than that of C10:0 or C12:0. (Norgren et al., 2020; St-Pierre et al., 2019) These processes allow MCTs to be quickly metabolized and converted into energy, permitting the partial replacement of LCTs in KDs and allowing for a greater carbohydrate intake while maintaining ketosis. (Miranda et al., 2012)

The MCFAs C8:0 and C10:0 are of particular interest because of their unique metabolic properties. They can circulate systemically and cross the blood-brain-barrier, where astrocytes and neurons can metabolize them into KBs. (Augustin et al.,

2018; Jensen et al., 2020; Nimbkar et al., 2022; Wlaź et al., 2015) Notably, their metabolism may be different depending on the cell type. In SH-SY5Y cells, C8:0 is preferably metabolized, inhibiting the oxidation of C10:0 and leading to its accumulation in the brain. (Khabbush et al., 2017) Although MCFAs are often considered capable of crossing the mitochondrial membranes independently of transport systems (Schönfeld & Wojtczak, 2016), evidence suggests partial reliance on the carnitine shuttle. Inhibition of CPT1 with etomoxir markedly reduced β-oxidation of C10:0 (95%) and C8:0 (34%) in human neuronal-like SH-SY5Y cells. These findings indicate, that the carnitine shuttle, and specifically CPT1, is necessary for the β-oxidation of C10:0 and partially required for the oxidation of C8:0 in neuronal-like cells. (Khabbush et al., 2017) However in mouse brain slices, C10:0 was preferably oxidized over C8:0, and this oxidation was not affected by etomoxir inhibited CPT1. Based on these results, C8:0 and C10:0 metabolism in brain tissue slices is independent of carnitine and CPT1 (Andersen et al., 2021), indicating possible cell- and tissue-specific differences in CPT1-dependence. Accordingly, MCFA oxidation and their dependence on carnitine appears to be tissue specific. While the liver and kidney can oxidize MCFAs independent of carnitine, the SkM and heart cannot import free FAs and rely on the carnitine-shuttle for mitochondrial import. (Pereyra et al., 2023)

Further distinctions exist between C8:0/C10:0 and C12:0 metabolism. Mice with impaired C12:0 oxidation (Sirtuin 5- and LCAD-knockouts), developed steatosis when fed a C12:0-rich diet from coconut oil, whereas MCAD-knockout mice on a C8:0/C10:0-rich diet did not. These findings may also imply that MCAD is not solely responsible for the oxidation of MCFAs such as C8:0 and C10:0. (Goetzman et al., 2020) Additionally, C8:0 and C12:0 activation may be mediated by different enzymes. Inside mitochondria, free MCFAs are activated by medium-chain acyl-CoA synthetases (ACSM1 and ACSM2), which show markedly higher reactivity with C8:0 compared to C12:0. In contrast, long-chain acyl-CoA synthetases (ACSLs), which activate FAs in the cytosol, are more reactive with C12:0 than with C8:0. Furthermore, C12:0 can partially be metabolized in peroxisomes. These findings suggest that C12:0 is metabolized through a distinct pathway, and is processed more similarly to LCFAs than MCFAs. (Goetzman et al., 2020)

Beyond their role as energy substrates, MCFAs also act as signaling molecules. In the cytosol, C8:0-C10:0 MCFAs can activate PPARγ, thereby regulating gene expression. (Huang et al., 2021; Liberato et al., 2012) In adipose tissue, PPARγ regulates adipogenesis and contributes to glucose and FA metabolism by regulating genes related to lipogenesis, FA transport and gluconeogenesis. (Hernandez-Quiles et al., 2021) In addition, PPARγ exerts anti-inflammatory effects by inhibiting NF-κB signaling and activating anti-inflammatory mediators. (Kytikova et al., 2020) The isoform PPARγ1 is expressed not only in adipose tissue but also in other tissues including the liver, SkM and immune cells. (Hernandez-Quiles et al., 2021)

MCTs may also activate AMPK through increased AMP levels (Huang et al., 2021), which subsequently activates PGC-1α, one of the main regulators of mitochondrial biogenesis. Several studies indicate that MCTs enhance mitochondrial oxidative activity and biogenesis while reducing oxidative stress, possibly through this pathway. (Huang et al., 2021; Popov, 2020) Mice fed an MCT-enriched diet performed better during exercise in a heated environment, with SkM demonstrating enhanced carbohydrate and FA metabolism. This was accompanied by increased mitochondrial biogenesis in SkM via activation of Akt (protein kinase B) and AMPK pathways. (Wang et al., 2018) Similarly in rats, a high-fat MCT-diet (74,3% C8:0 of FAs) indicated enhanced mitochondrial oxidative capacity in both fast- and slow-twitch SkM fibers. (Ishizawa et al., 2015) Loss of AMPK activity reduces MCFA oxidative capacity by up to 45% in mouse cardiomyocytes, while LCFA oxidation remains unaffected, highlighting the importance of AMPK activation in MCFA metabolism. (Stride et al., 2012)

In mouse myoblasts, C8:0 promoted mitophagy through the PINK1-Parkin pathway and enhanced the expression of PGC-1α and DRP1, leading to increased OXPHOS and reduced ROS *in vitro*. These findings suggest, that C8:0 may improve mitochondrial quality control and promote the maturation of SkM. (Nishida et al., 2024) Consistently, dietary C8:0 supplementation in mice increased endurance capacity and upregulated mitochondrial biogenesis pathways via AMPK activation and subsequent induction of PGC-1α and OXPHOS. This is associated with a shift in muscle fiber composition toward a more oxidative type with higher mitochondrial content. (Charlot et al., 2022; Wallace et al., 2021) In human neuronal and

fibroblast cells, C10:0 too has been shown to increase mitochondrial biogenesis, possibly as a downstream effect of binding to and activating PPARγ. (Hughes et al., 2014; Kanabus et al., 2016; Malapaka et al., 2012)

Collectively, these findings suggest that KDs and MCFAs, particularly C8:0, may help maintain or restore SkM health. By increasing mitochondrial biogenesis and antioxidative capacity, long-term KDs and C8:0 may help mitigate sarcopenia. (Nishida et al., 2024; Wallace et al., 2021) Furthermore, an MCT-KD has been shown to attenuate muscle degeneration in mice with Duchenne muscular dystrophy. (Fujikura et al., 2021)

MCTs and MCFAs have also been suggested to promote thermogenesis in mice and humans, however the underlying mechanisms are not yet fully understood. (Huang et al., 2021)

7. Brown adipose tissue and skeletal muscle

The BAT and SkM may appear fundamentally different, yet they share several important similarities. Both tissues are rich in mitochondria, reflecting their high capacity for energy production. Their mitochondrial proteomes are also very similar, with both expressing high levels of OXPHOS-related enzymes such as pyruvate dehydrogenase kinase and CPT. (Pani et al., 2022) Markedly in humans, the mitochondrial respiratory capacity of BAT and SkM has been shown to be comparable. (Porter et al., 2016) Developmentally, BAT and SkM both originate from Myf5+ progenitor cells, which makes BAT more closely related to SkM than to white adipose tissue (WAT). Supporting this developmental link, brown adipocyte-like cells have even been identified within SkM. (Pani et al., 2022) It has further been proposed, that a direct cross-talk may occur between BAT and SkM. (Bal et al., 2017)

Both tissues are play central roles in thermogenesis, although their contributions differ between species. In adult humans, cold-induced heat production predominantly relies on SkM through shivering thermogenesis. In contrast, mice depend more heavily on non-shivering thermogenesis mediated by BAT. These interspecies differences highlight the need for caution when extrapolating findings from mice to humans. (Marlatt et al., 2018)

Adipose tissue is not only a storage site for energy, it is also metabolically active, especially BAT. There are three types of adipose tissue in mammals: WAT, BAT and beige or brite adipose tissue (bAT). While WAT primarily stores energy in the form of fat, BAT burns energy and generates heat through non-shivering thermogenesis, uncoupling mitochondrial respiration from ATP production via uncoupling protein 1. Beige adipocytes can emerge within WAT through a process known as “browning”, enhancing thermogenic potential. (Cedikova et al., 2016)

Brown adipocytes are characterized by a high amount of larger mitochondria, along with numerous small lipid droplets, whereas white adipocytes have smaller, elongated mitochondria and a single large lipid droplet. (Frontini & Cinti, 2010) Brown preadipocytes exhibit gene expression patterns similar to myocytes, while both brown and white primary preadipocytes display distinct expression profiles. This may explain why brown adipocytes, like the SkM fibers, are involved in lipid catabolism rather than storage. (Timmons et al., 2007)

The distribution of BAT in the human body varies depending on sex, age and environmental influences such as ambient temperature and physical activity. (Frontini & Cinti, 2010) Although similar, murine BAT only partially reflects the characteristics of human BAT. Human BAT is thought to more closely resemble the bAT found in rodents than classical BAT. (Pani et al., 2022) When the ambient temperature drops below the thermoneutral zone of the body, BAT is activated to maintain body temperature. Because thermoneutrality in mice occurs at around 30°C ambient temperature, mice use roughly 20% of total energy expenditure for thermoregulation in standard housing temperatures (20-23°C). (Cannon & Nedergaard, 2004; Farooqi & Xu, 2024)

BAT was long thought to be present only in newborns or to play a minimal role in adults. However, more recent evidence has shown that BAT is indeed present and metabolically active in adult humans, although only in small amounts and its activity declines with age. (Frontini & Cinti, 2010; Saito, 2013)

Active BAT burns large amounts of glucose and lipids. Although it accounts for only a small percentage of the total body mass, BAT consumes more than half of the body’s oxygen uptake during peak thermogenesis. (Cannon & Nedergaard, 2004)

Its recruitment is naturally induced by cold exposure. In mice, endurance exercise can even induce the browning of WAT and may also stimulate classical BAT depots (Vosselman et al., 2015), but comparable effects have not been demonstrated in humans. Pharmacological activation of BAT is theoretically possible via stimulation of the sympathetic nervous system, for example through β_3-adrenergic receptor agonists. Nevertheless, their clinical application remains limited due to adverse effects on the cardiovascular and muscular systems. Targeting the activation of BAT has been proposed as a potential therapeutic strategy for obesity. However, current evidence is insufficient to support its clinical application. Nonetheless, BAT activation may have other beneficial effects, including improved glucose and insulin metabolism as well as cardioprotective effects. (Marlatt et al., 2018)

The activation of BAT through cold exposure has been suggested to suppress tumor growth. It was demonstrated that mice exposed to 4°C exhibited increased glucose uptake, enhanced lipid metabolism and reduced tumor growth. (Seki et al., 2022) However, corresponding evidence in humans is currently lacking.

Skeletal muscle, by contrast, is a heterogenic tissue composed of muscle fibers with different metabolic demands. The types of SkM fibers have distinct energy requirements due to their varying metabolic activity. Slow-twitch fibers support prolonged endurance activities and primarily rely on oxidative metabolism, while fast-twitch fibers are adapted for short and intense activities and can exhibit a spectrum ranging from highly oxidative to highly glycolytic metabolism. (Zumbaugh et al., 2022) To meet diverse exercise demands, SkM must remain highly adaptable, particularly through regulating mitochondrial content and adjusting energy production capacity.

8. Experiment setup

In this study, the house mouse (*Mus musculus*) is employed as a model organism to investigate metabolic processes, with the aim of translating the observed effects to human physiology. *Mus musculus* is widely used in medical research to study the mechanisms underlying human diseases, owing to its small size, rapid reproductive cycle, cost-effectiveness, and the availability of genetic modification techniques. (Rydell-Törmänen & Johnson, 2019)

Although the mouse genome is very similar to that of humans, differences in cis-regulatory elements, gene expression patterns and tissue specific transcriptional profiles are documented. (Yue et al., 2014) Nevertheless, mice remain an excellent model organism for investigating the metabolism, as key metabolic pathways such as glucose and lipid metabolism are highly preserved between mice and humans. However, notable physiological differences such as their higher basal metabolic rate and thermogenesis remain, which affects the adaptation to dietary interventions. (Pap et al., 2016) For instance, to induce ketosis in mice, dietary carbohydrates must be restricted to less than 1% of the total energy intake, whereas in humans it can be sustained with intakes of up to 20%. (Nelson et al., 2023) This underlines the complications of translating such experimental results to humans.

Gene expression is a complex, multilayered process modulated by various regulatory mechanisms that determine whether a gene is activated or silenced. Nutrients and environmental stimuli can dynamically influence gene expression both in the short and long term. Quantitative real-time polymerase chain reaction (qPCR) provides a simple and cost-effective method for quantifying mRNA levels and identify transcriptional adaptations in response to dietary interventions. However, post-translational modifications, enzyme regulation, and protein degradation further modulate protein function, highlighting that mRNA expression does not always correlate directly with biological activity.

9. Target genes

Eleven genes were selected for analysis in this study, all of which are orthologous to their human counterparts, indicating a high degree of evolutionary conservation between species. Their functions are therefore presumed to be largely comparable in mice and humans. (O'Leary et al., 2016; The Alliance of Genome Resources Consortium, 2024)

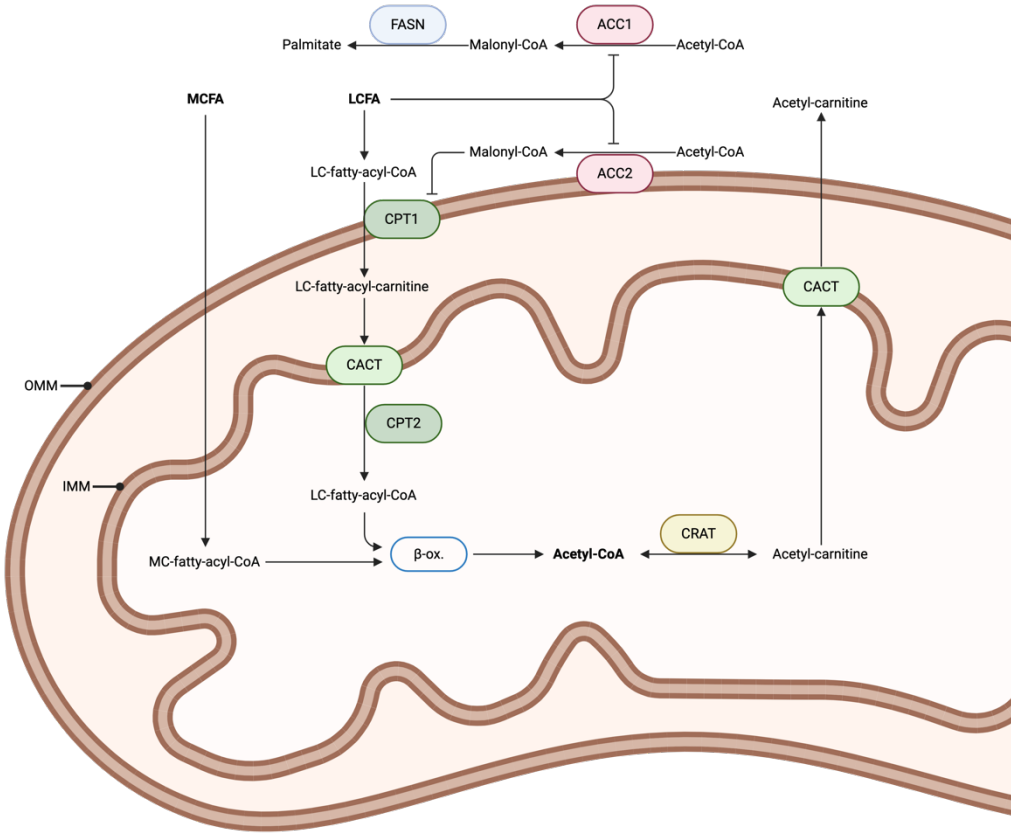

Figure 1: Simplified metabolic pathways in mitochondria of mice and humans of acetyl-CoA carboxylase alpha (ACC1), acetyl-CoA carboxylase beta (ACC2), mitochondrial carnitine/acylcarnitine carrier protein (CACT), carnitine O-palmitoyltransferase 1 (CPT1), carnitine O-palmitoyltransferase 2, mitochondrial (CPT2), carnitine O-acetyltransferase (CRAT) and fatty acid synthase (FASN), lines with arrows indicate transport/activation, lines with bars indicate inhibition, β-ox. = β-oxidation, CoA = Coenzyme A, IMM = inner mitochondrial membrane, OMM = outer mitochondrial membrane, LCFA = long-chain fatty acid, MCFA = medium-chain fatty acid, created in https://BioRender.com.

9.1 Acaca and Acacb

The murine *Acaca* (acetyl-Coenzyme A carboxylase alpha) and *Acacb* (acetyl-Coenzyme A carboxylase beta) are orthologous to the human *ACACA* (acetyl-CoA carboxylase alpha) and *ACACB* (acetyl-CoA carboxylase beta) genes respectively. (O'Leary et al., 2016) In mammals, two isoforms of ACCs exist: acetyl-Coenzyme A carboxylase alpha (ACC1), encoded by *Acaca*, and acetyl-Coenzyme A carboxylase beta (ACC2), encoded by *Acacb*. The expression patterns of ACC isoforms differ markedly between rodents and humans. In rodents, ACC1 is highly expressed in WAT, whereas in humans, ACC2 expression exceeds that of ACC1 in

this tissue. In SkM, both isoforms appear to be expressed at comparable levels. (Castle et al., 2009; Wang et al., 2022)

ACCs regulate FAS and FAO by catalyzing the carboxylation of acetyl-CoA to malonyl-CoA. As this represents the first rate-limiting step in *de novo* FAS, ACCs are key regulators of lipid metabolism and storage. Moreover, malonyl-CoA exerts an inhibitory effect on CPT1, making it a crucial modulator of β-oxidation. Although both isoforms catalyze the same reaction, their different subcellular localizations result in distinct functional effects. The malonyl-CoA produced by ACC1 in the cytosol is channeled into FAS, whereas malonyl-CoA produced by ACC2 at the OMM acts as an allosteric inhibitor of CPT1. In humans, ACC2 is thought to play a greater role in regulating β-oxidation than in FAS. However, the precise physiological role of ACC2 remains to be fully clarified. (O'Leary et al., 2016; Wang et al., 2022)

Food intake and energy status strongly influence ACC expression and activity. During times of nutrient abundance, ACC expression and activity are upregulated, while their activity is reduced during energy scarcity. Transcription factors such as sterol regulatory element-binding proteins (SREBP1a and SREBP1c) and ChREBP (carbohydrate response element-binding protein) are activated in response to a high-carbohydrate diet, leading to increased transcription of ACC genes. Activated AMPK inhibits ACC activity and thereby suppresses FAS. LCFA-CoAs also directly inhibit ACCs, increasing FAO by reducing the malonyl-CoA inhibitory effect on CPT1. Conversely citrate, an intermediate of the TCA cycle, can allosterically activate ACC1. (Tong, 2005; Wang et al., 2022) Notably, because ACC activity is frequently regulated at the post-transcriptional level, its mRNA expression may not directly reflect its enzymatic activity.

The physiological importance of ACC isoforms has been highlighted in genetic models. *Acc1*$^{-/-}$ mice are embryonically lethal (Abu-Elheiga et al., 2005), underscoring the essential role of ACC1 in early development. In contrast, *Acc2*$^{-/-}$ mice display a normal lifespan, exhibit increased β-oxidation and accumulate less fat compared to the wild type mice. In these mice, enhanced β-oxidation results from reduced malonyl-CoA levels and the consequent alleviation of CPT1 inhibition. (Abu-Elheiga et al., 2001, 2003)

Malonyl-CoA not only acts as a metabolic intermediate but also as an energy sensor and signaling molecule. In addition to its well-established role in inhibiting β-oxidation, malonyl-CoA can signal to mechanistic target of rapamycin complex 1 (mTORC1), reflecting the cells capacity for FAS. ACC1 and FASN have been shown to form a complex with mTORC1. When malonyl-CoA accumulates, due to hyperactivation of ACC1 or reduced FASN activity, it may bind to proximal mTORC1, competing with ATP for binding, and suppress its activity. This regulatory mechanism is evolutionarily conserved and has been observed as far back as yeast cells. (Nicastro et al., 2023)

Moreover, mitochondrial architecture has recently been recognized as an important determinant of FA import and oxidation. The size of mitochondria and the conformation of their membrane directly affects the sensitivity of CPT1 to malonyl-CoA. Elongated mitochondria exhibit greater CPT1 sensitivity, leading to stronger inhibition of CPT1 and decreased FAO. In contrast, smaller and fragmented mitochondria exhibit more highly curved membranes, rendering CPT1 less sensitive to malonyl-CoA and thereby facilitating increased FA import and oxidation rates. (Ngo et al., 2023)

9.2 Fasn

The murine *Fasn* (fatty acid synthase) is orthologous to human *FASN* (fatty acid synthase) and both genes encode for the FASN enzyme (The Alliance of Genome Resources Consortium, 2024), which is essential for FAS. FASN catalyzes the *de novo* synthesis of palmitic acid (C16:0) from malonyl-CoA in the cytosol through seven enzymatic steps. The resulting long-chain saturated FAs can be further elongated, desaturated, incorporated into triglycerides or phospholipids, integrated into cellular membranes, function as signaling molecules, or be oxidized to generate energy. (Lage et al., 2008)

Similar to *Acaca* and *Acacb*, *Fasn* expression is regulated by cellular energy status and nutrient availability. Under energy-deprived conditions, activated AMPK downregulates *Fasn* expression and thereby limiting lipogenesis. (Lage et al., 2008) mTORC1 regulates *Fasn* expression indirectly by modulating SREBP, one of the main transcription factors that control Fasn expression. (Nicastro et al., 2023)

Under normal physiological conditions, *de novo* FAS is typically low as dietary intake provides sufficient FAs. Consequently, *Fasn* overexpression is associated with metabolic disorders such as obesity, diabetes, and cancer. (Rittner et al., 2020) Moreover, FASN protein levels increase during the induction of cellular senescence in both mouse and human cells, whereas its inhibition prevented the onset of senescence, suggesting a functional role of FASN in this process. (Fafián-Labora et al., 2019)

9.3 Acadm

The murine *Acadm* (acyl-Coenzyme A dehydrogenase, medium chain) is orthologous to the human *ACADM* (acyl-CoA dehydrogenase medium chain) and encodes for the ACADM enzyme, also known as MCAD. ACADM is a key enzyme in β-oxidation. It belongs to the acyl-CoA dehydrogenase family and exhibits optimal activity toward acyl-CoAs with chain lengths of 6-12 carbon atoms in mice and 4-12 carbon atoms in humans. (Mason et al., 2023; O'Leary et al., 2016)

Individuals with medium-chain acyl-CoA dehydrogenase deficiency (MCADD) typically exhibit hypoglycemia, reduced levels of acetyl-CoA, and an accumulation of MCFAs and acyl-carnitines. In some cases this condition can be fatal. (Mason et al., 2023; O'Leary et al., 2016) However, certain individuals remain asymptomatic despite impaired MCAD function. (Martines et al., 2019) Due to their overlapping substrate ranges, the isozymes SCAD and LCAD are capable of partially compensating for the loss of MCAD function. Nonetheless, Martines et al. (2019) demonstrated, that octanoyl-CoA oxidation is significantly reduced in MCAD-deficient mice. Furthermore, they reported no compensatory upregulation of SCAD or LCAD, as protein expression levels remained unchanged compared to wild-type controls.

9.4 Crat

Murine *Crat* (carnitine acetyltransferase) is orthologous to human *CRAT* (carnitine O-acetyltransferase) and encodes for the carnitine O-acetyltransferase (CRAT). Multiple transcript variants exist through alternative splicing, resulting in distinct

isoforms that may have different cellular locations. (O'Leary et al., 2016; The Alliance of Genome Resources Consortium, 2024)

Mammalian CRAT has been found in several cellular compartments, including the mitochondrial matrix, the peroxisomal matrix, the endoplasmic reticulum, the nucleus and in the cytosol. However, the precise roles and subcellular localizations of these isoforms have not been defined yet. (Dambrova et al., 2022; Volpicella et al., 2025)

Mitochondrial CRAT plays a key role in regulating acetyl-CoA homeostasis and overall cellular energy metabolism by catalyzing the reversible transfer of acetyl groups between acetyl-CoA and acetyl-carnitine. This reaction prevents the accumulation of acetyl-CoA and provides a buffering system for acetyl-CoA availability. Moreover, CRAT has been proposed to influence gene expression by regulating the pool of acyl groups available for histone acetylation. (Dambrova et al., 2022; Volpicella et al., 2025) Proper CRAT function is crucial for metabolic health, as CRAT silencing *in vitro* causes mitochondrial dysfunction, inflammation and senescence. Additionally, reduced CRAT is associated with skin aging. (Song et al., 2023)

9.5 Fis1

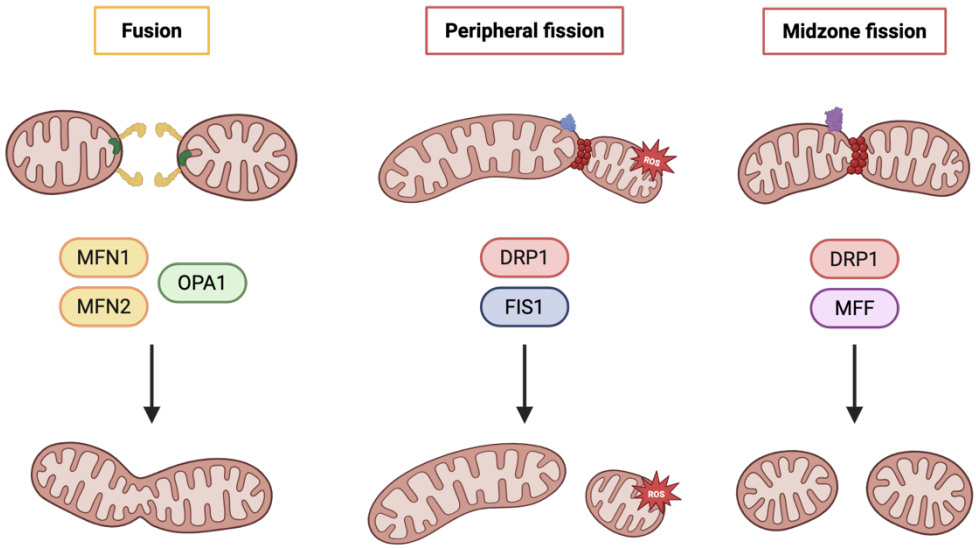

Figure 2: Fusion and fission of mitochondria: dynamin-1-like protein (DRP1), fission, mitochondrial 1 (FIS1), mitochondrial fission factor (MFF), mitofusin 1 (MFN1), mitofusin 2 (MFN2), OPA1 mitochondrial dynamin like GTPase (OPA1), reactive oxygen species (ROS), based on Tábara et al. (2024) , created in https://BioRender.com

The murine *Fis1* (fission, mitochondrial 1) gene is orthologous to human *FIS1* (fission, mitochondrial 1) and encodes for the FIS1 protein, which is located in the OMM and peroxisomal membrane. (The Alliance of Genome Resources Consortium, 2024) Three transcript variants and their corresponding isoforms have been described. (O'Leary et al., 2016)

FIS1 acts as a regulator of mitochondrial peripheral fission by recruiting DRP1 to mitochondria. In addition, it is responsible for the recruiting of lysosomes and mitochondria-lysosome tethering. (Kleele et al., 2021; Liesa & Shirihai, 2013; Tábara et al., 2024) In animal models, *Fis1* overexpression typically results in increased fission and *Fis1* knockout in increased elongation of mitochondria. Additionally, FIS1 is involved in apoptosis and mitophagy as well as fission of peroxisomes. (Ihenacho et al., 2021)

In SkM, FIS1 contributes to mitochondrial quality control in slow muscle fibers both at rest and during exercise-induced stress *in vivo*. In *Fis1* knockout mice, slow-twitch muscle fibers exhibit mitochondrial hyperfusion, respiratory chain impairment and elevated mitophagy. (Z. Zhang et al., 2019) Still, FIS1 function in humans is still not completely understood. (Ihenacho et al., 2021) The incomplete amplification of *Fis1* transcript variants and the limited understanding of their distinct functions should be considered when interpreting the results.

9.6 Mfn1 and Mfn2

The murine *Mfn1* (mitofusin 1) and *Mfn2* (mitofusin 2) genes are orthologous to human *MFN1* (mitofusin 1) and *MFN2* (mitofusin 2). (The Alliance of Genome Resources Consortium, 2024) They encode for the enzymes MFN1 and MFN2 respectively, which are essential regulators of mitochondrial OMM fusion.

The primary role of MFN1 is the fusion of the OMM, whereas MFN2 not only contributes to this process but also fulfills additional functions, including the enhancement of ATP production and the maintenance of mitochondrial quality control. MFN2 facilitates the connection between the endoplasmic reticulum and mitochondria, thereby promoting calcium transfer into mitochondria and optimizing ATP production. Furthermore, MFN2 regulates autophagy and mitophagy through the PINK1 (PTEN-induced kinase 1)-Parkin pathway, contributing to the removal of dysfunctional mitochondria. (Zanfardino et al., 2025) Additionally, MFN2 is required for mitochondrial transport along axons, highlighting its importance in neuronal function. (Misko et al., 2010)

Together, MFN1 and MFN2 are crucial for mitochondrial function, not only through their regulation of mitochondrial morphology, but also by maintaining mtDNA levels, thereby contributing to the regulation of glucose homeostasis in pancreatic β-cells. (Sidarala et al., 2022)

9.7 Opa1

The murine *Opa1* (OPA1, mitochondrial dynamin like GTPase) gene is orthologous to human *OPA1* (OPA1 mitochondrial dynamin like GTPase) and encodes for the optic atrophy protein 1 in humans and optic atrophy 1 homolog (OPA1) protein in

mice. (The Alliance of Genome Resources Consortium, 2024) The primer used in this study targets all five isoforms collectively. However, this approach is not optimal, as the individual isoforms have distinct functions, which limits the interpretability of the results. (Austin et al., 2022)

OPA1 is a key mediator of IMM fusion, complementing MFN1 and MFN2. (Tábara et al., 2024) Beyond its role in mitochondrial fusion, OPA1 optimizes OXPHOS, reduces ROS generation and enhances ATP production by regulating cristae morphology and facilitating the formation of respiratory chain supercomplexes. Conversely, OPA1 dysfunction leads to increased ROS levels which can activate PGC-1α. (Zanfardino et al., 2025)

Mitochondrial fusion enables the exchange of metabolites and mitochondrial DNA (mtDNA) between organelles and is contingent on the mitochondrial membrane potential ($\Delta\psi_m$). Mitochondria with higher $\Delta\psi_m$ are more likely to fuse, whereas those with reduced $\Delta\psi_m$ are excluded from this process. This selectivity is closely linked to OPA1, as mitochondria with low $\Delta\psi_m$ and diminished OPA1 fail to undergo fusion. As a result, a sub-population of depolarized non-fusing mitochondria is formed, which is subsequently targeted for autophagic degradation. (Twig et al., 2008)

9.8 Trp53

The murine *Trp53* (transformation related protein 53) gene is orthologous to human *TP53* (tumor protein p53) and encodes for the tumor suppressor p53. (O'Leary et al., 2016) In mice, four known isoforms can arise from the *Trp53* gene, the canonical full length Mp53α, as well as the Mp53AS, MΔ41p53α and Mp53ψ isoforms. Transcript variant 1 encodes the longer isoform (a): Mp53α (Trp53 (l)). Transcript variant 2 encodes the shorter isoform (b): Mp53AS (Trp53 (s)). Due to alternative splicing of the 3' exon/intron 10, the (b) isoform has a shorter and different C-terminus. Mp53α and Mp53AS are homologous to human full length p53α (Joruiz & Bourdon, 2016; O'Leary et al., 2016) and human p53β (Wolf et al., 1985) respectively. In humans, twelve isoforms of p53 have been identified. They regulate gene expression and are usually expressed simultaneously. Because p53 acts as a tetramer, its various isoforms interact with one another, and the specific combination

of isoforms expressed leads to distinct functional outcomes within cells. (Guo et al., 2024; Joruiz & Bourdon, 2016) The impact of these isoforms likely contributes to the diverse activities attributed to p53. (Joruiz & Bourdon, 2016)

P53 is known as a master regulator with highly complex and context-dependent functions that are not yet fully understood, particularly when considering the full spectrum of its isoforms. It influences cellular metabolism through its role as a transcription factor. It regulates gene expression, microRNAs and long non-coding RNAs and post-translationally modifies proteins. Through its regulation of major signaling pathways such as mTOR, AMPK, and NF-κB, p53 exerts control over core metabolic processes. It contributes to the regulation of energy metabolism, influencing glucose uptake, amino acid turnover, and lipid processing by inhibiting FAS and stimulating FAO. (Hamsanathan & Gurkar, 2022; Joruiz & Bourdon, 2016; Temaj et al., 2024)

The p53 is activated in response to various cellular stress signals, including DNA-damage, hypoxia and nutrient deprivation. It functions as a tumor suppressor by regulating DNA repair, apoptosis and autophagy. However, chronic activation of p53 can contribute to the induction of cellular senescence. (Hamsanathan & Gurkar, 2022; Temaj et al., 2024) Conversely, loss of p53 function promotes chromosomal instability, as affected cells undergo senescence or apoptosis. (He et al., 2018)

Beyond its role in genome stability, p53 also influences mitochondrial dynamics. It modulates mitochondrial morphology through the PKA (protein kinase A)-DRP1 pathway, where inhibition of DRP1 and increased intracellular ROS during senescence promote mitochondrial dysfunction by increased mitochondrial elongation. (Kim et al., 2020) In mice, KD feeding induced cellular senescence in the heart, kidney, and other organs via AMPK activation and caspase-2-mediated inactivation of mouse double minute 2, leading to p53 accumulation and subsequent p21 activation. (S.-J. Wei et al., 2024)

Notably, p53 function is regulated by post-translational modifications, therefore mRNA data must be interpreted with caution. (Hamsanathan & Gurkar, 2022; Joruiz & Bourdon, 2016)

10. Materials

10.1 Mice and diets

Mouse BAT and SkM cDNA samples were provided by my supervisor Dr. Sternberg. The samples originated from the study described in Sternberg et al. (2023).

All animal experiments were approved by the Austrian national authority according to §§ 26ff. of the Animal Experiments Act, Tierversuchsgesetz 2012-TVG 2012 (BMWFW-66.006/0008-V/3b/2018). All procedures were in alignment with the directive 2010/63/EU of the European Parliament on the protection of animals used for scientific purposes.

Male C57/BL6NRJ mice were housed at a constant ambient temperature of 23°C and regulated humidity under a standard 12h/12h-dark/light cycle with access to water *ad libitum*. Throughout the study, all mice were kept under the same housing conditions and fed with standard chow *ad libitum* for the first 12 weeks. Then they were randomly assigned to one of five dietary groups, each consisting of eight mice.

Mice were fed according to the diet compositions described in Gregor et al. (2022) and Sternberg et al. (2023). The control group was continued to be fed with standard chow *ad libitum* (SD) for eight weeks. The LCT-based diet (LCT), comprised 74,6% fat, 8,1% protein and 1% sugar and was followed for eight weeks *ad libitum*. The LCT/MCT-diet (LCT/MCT) was similar to the LCT-diet but featured a different FA composition, containing a ratio of 70% LCT and 30% MCT of total fat, also administered for eight weeks *ad libitum*. Mice under caloric restriction diet (CR) were fed once per day with 80% of the energy of the SD-mice for the last two weeks. Mice under intermittent fasting diet (IF) were fed under a 24-hour cycle of complete fasting and *ad libitum* refeeding for the last two weeks. At the age of 20 weeks, all mice were sacrificed via anesthesia overdose and tissues were collected.

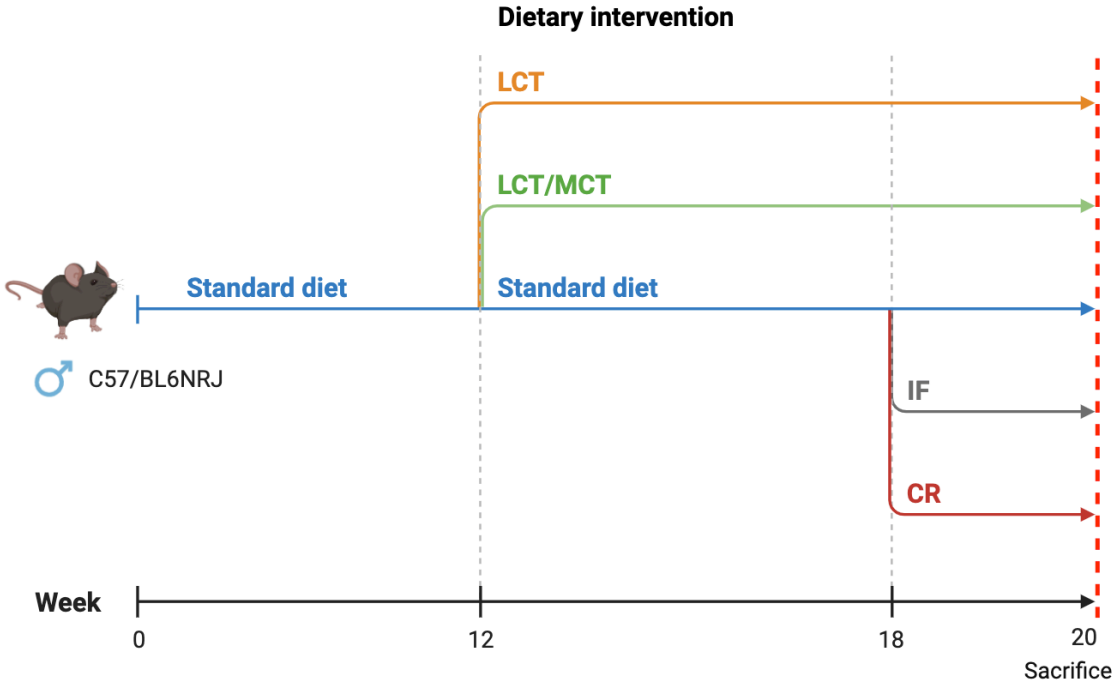

Figure 3: Mice dietary interventions timeline, created in https://BioRender.com

Table 1: Diets		
Diet	Product number	Company
SD	S9139-E028	ssniff
LCT	S9139-E025	ssniff
LCT/MCT	S9139-E032	ssniff
IF	V153x R/M-H auto	ssniff
CR	V153x R/M-H auto	ssniff

10.2 Chemicals and kits

Table 2: Kits and chemicals		
Kits and chemicals	Product number	Company
Chloroform	n. a.	Sigma-Aldrich
Isopropanol	n. a.	Sigma-Aldrich
Glycogen	AM9510	Thermo Fisher Scientific

NF-H2O	E476-500ML	VWR
Agarose	A6013-5G	Sigma-Aldrich
50 x TAE-Electrophoresis Buffer	B49	Thermo Fisher Scientific
6 x DNA loading dye	R0611	Thermo Fisher Scientific
Gene ruler 100 bp DNA Ladder	SM0241	Thermo Fisher Scientific
peqGreen DNA/RNA Dye	37-5000	peqlab
2 x ChamQ Universal SYBR qPCR Master Mix	Q711-03	Vazyme
RNase AWAY	R323-01-AA	Vazyme

10.3 Primer

Primer pairs were ordered from Microsynth Austria GmbH.

Table 3: All primer pairs

Primer	Direction	Sequence 5'-3'	Primer length [bp]	Amplicon length [bp]	Efficiency [%]	Company
mAcaca(1)	Forward	GCCGCCAGCCTGAGTTCTTT	20	140	105,82	Microsynth
	Reverse	CGGGAGTGCTGGTTTAGCTCC	21			
mAcaca(2)	Forward	GCCGCCAGCCTGAGTTCTT	19	112	93,06	Microsynth
	Reverse	TGGCCAACGGAGATGGTTCA	20			
mAcacb	Forward	CTACAAGACGGCGCAGGTCA	20	128	103,49	Microsynth
	Reverse	AGGCGCCAAACTTCAGCATC	20			
mAcadm(1)	Forward	TTCCGGAAAGTTGCGGTGGC	20	84	113,5	Microsynth
	Reverse	CCCCTGTACACCCATACGCC	20			
mAcadm(2)	Forward	GGGGGAAAGGCCAACTGGTAT	21	151	101,18	Microsynth
	Reverse	AGCATCGCTGGCCCATGTTT	20			
mCrat	Forward	TGACTCGGCGACCTTGAACCTA	22	168	107,66	Microsynth
	Reverse	CCCAGGGGTTTTACCACGGTTC	22			
mFasn(1)	Forward	AACACGATCTGGTGCTGCCC	20	105	99,79	Microsynth
	Reverse	TGGGGGCTGTCGTGTCAGTA	20			
mFasn(2)	Forward	CAACCACCCTCTGGGCATGG	20	152	103,48	Microsynth
	Reverse	TGAGGGGCTTCACGACTCCA	20			
mFis1	Forward	GCTGGTTCTGTGTCCAAGAGCA	22	144	94,51	Microsynth
	Reverse	GACATAGTCCCGCTGTTCCTCT	22			
mHprt(1)	Forward	CAAACTTTGCTTTCCCTGGT	20	101	101,37	Microsynth
	Reverse	TCTGGCCTGTATCCAACACTTC	22			
mHprt(2)	Forward	GCAGTCCCAGCGTCGTGATTAG	22	147	89,99	Microsynth
	Reverse	TGTGATGGCCTCCCATCTCCT	21			
mMfn1	Forward	CCAGGTACAGATGTCACCACAG	22	149	101,35	Microsynth

	Reverse	TTGGAGAGCCGCTCATTCACCT	22			
mMfn2	Forward	TCCCTCTGACACCTGCCAAC	20	155	90,94	Microsynth
	Reverse	TGCCTTCCACACCACTCCTC	20			
mOpa1(1)	Forward	TCCACCACAGGAAGCTCAAGAAATC	25	141	102,34	Microsynth
	Reverse	TTTTCCCAGCACTCTGATCTCCAAC	25			
mOpa1(2)	Forward	CAGCTGGCAGAAGATCTCAAGAAA	24	189	107,53	Microsynth
	Reverse	GAAAAGGGTAGAACGGGAGGAAAG	24			
mRpl4	Forward	GTATGGCACTTGGCGGAAGG	20	124	91,57	Microsynth
	Reverse	TGCTCGGAGGGCTCTTTGG	19			
mTbp	Forward	CTACCGTGAATCTTGGCTGTAAAC	24	131	102,36	Microsynth
	Reverse	AATCAACGCAGTTGTCCGTGGC	22			
mTrp53(1)	Forward	TCCGAAGACTGGATGACTGCC	21	132	128,83	Microsynth
	Reverse	GCAGTGAGGTGATGGCAGGA	20			
mTrp53(2)	Forward	CTCCGAAGACTGGATGACTGCC	22	133	141,12	Microsynth
	Reverse	GCAGTGAGGTGATGGCAGGA	20			
mTrp53(3)	Forward	GCAGGGCTCACTCCAGCTAC	20	124	100,23	Microsynth
	Reverse	GTGATGGGGACGGGATGCAG	20			
mTrp53(4)	Forward	CAGGGCTCACTCCAGCTACC	20	113	98,5	Microsynth
	Reverse	CGGGATGCAGAGGCAGTCAG	20			
mTrp53(5)	Forward	TTCCGGGAGCTGAATGAGGC	20	93	96,3	Microsynth
	Reverse	TCTAGGCTGGAGGCTGGAGTG	21			
mTrp53(6)	Forward	GCTCACTCCAGCCTCCAGC	19	71	104,04	Microsynth
		GGGAGCTAGCAGTTTGGGCT	20			

11. Methods

11.1 Primer design

Primer pairs for relevant genes used in previous studies with published and validated sequences were selected for ordering and subsequent testing. The remaining primer sequences were designed using the NCBI Primer-Blast. (Ye et al., 2012) When multiple transcript variants were existent, primers were designed to cover as many of them as possible.

In the case of *Trp53*, the expression of the two predominant variants, namely Mp53α (Trp53 (l)) and Mp53AS (Trp53 (s)), was analyzed. Six primer pairs were designed: one pair targeting both isoforms simultaneously, and two specific to each individual variant. During primer validation using a cDNA serial dilution series, the primer pairs designed to amplify both variants simultaneously produced atypical amplification curves. This suggested suboptimal primer performance or

interference between targets when amplified together. Consequently, the transcript variants were analyzed separately.

Five CRAT isoforms are described, however the primer used in this study only amplifies the a, c and e variants. Similarly, for *Fis1,* the primer targets only isoforms 1 and 2, as designing a primer covering all three isoforms proved methodologically challenging. These limitations may affect data accuracy and should be taken into account when interpreting the results.

Primer melting temperatures (T_m) were set to min = 60°C, opt = 63°C and max = 66°C. The Max PCR product size was reduced to 200. Primers were designed to span an exon-exon junction to minimize the binding to possible gDNA residues. For each target, two primer pairs were ordered. After testing, the primer pair demonstrating superior amplification efficiency and Ct-confidence area together with well-defined melting curves was selected for subsequent experiments.

11.2 Primer validation

After arrival the primers were diluted according to manufacturer's instructions to 100 µM and again diluted for a final concentration of 10 µM. Primer testing was conducted to assess their amplification efficiency and to establish the appropriate sample dilution. To evaluate primer efficiency, qPCR was performed. Each primer was tested in triplicates using a serial dilution of pooled mouse liver and BAT cDNA samples.

Initially, the cDNA was diluted 9 times, each time 1:2 with nuclease free H_2O for a total of nine dilutions. Primers Mfn1, Mfn2, Opa1 (1), Fis1 and Crat were tested. On a 384-well plate, 3 µl of primer was dispensed into each well. Then a master mix containing 5 µl ChamQ and 2 µl of the diluted cDNA for each well was added for a total of 10 µl per well. After closing the plate with sealing tape it was briefly centrifuged for 30 seconds at 400 rpm to get rid of any air bubbles on the bottom. This experiment was invalid due to the cDNA not being diluted enough and causing unsatisfactory results. Subsequently, the cDNA was first diluted 1:10 with nuclease free H_2O and then diluted 1:3 nine times for a total of 10 dilutions. The qPCR was performed as before with the same primers. This time the dilutions proved to be suitable and all the other primers were tested in this manner.

All qPCR experiments were performed by a QuantStudio 6 Flex Real-Time PCR system (Thermo Fisher Scientific) in a 384-well format with the following run method:

Table 4: qPCR run method

	Hold stage	PCR stage			Melt curve stage		
Cycles	1	40			1		
Steps		Denaturation	Annealing	Elongation			
Temperature [°C]	95	95	62	72	95	60	95
Time [minutes]	03:00	00:10	00:20	00:20	00:15	01:00	00:50
Increments [°C/s]	1,9	1,9	1,6	1,6	1,9	1,6	0,5

By creating a standard curve plotting C_t on the y-axis and the decadic logarithm of the dilution factor on the x-axis, the slope of the standard curve and primer efficiency were calculated for each primer (E = -1+10(-1/slope)).

11.3 Gel electrophoresis

To check if the amplicons have the right size a gel electrophoresis was performed. A 2% agarose gel was made by dissolving 2 g agarose with 110 ml 1 x TAE buffer (Tris-acetate EDTA) and boiling in the microwave until the solution was clear. Then 5 µl peqGreen was mixed in. The gel was poured in a running chamber with two combs. After the Gel solidified it was put into the electrophoresis chamber with 1 x TEA buffer until the gel was sufficiently covered. 1 µl loading dye was mixed with 5 µl of each sample on parafilm and then loaded into the gel pockets, as well as 3 µl GeneRuler 100 bp DNA ladder in the first, middle and last pockets to approximate the product size. The gel electrophoresis was carried out at 80 volts for a duration of 75 minutes.

11.4 qPCR of samples

With the cDNA samples of SkM and BAT, qPCR was done for each diet and tissue. The genes ribosomal protein L4 (*Rpl4*) and TATA box binding protein (*Tbp*) were used for housekeeping. Samples and non-template control were tested in duplicates.

On a 384-well plate, 3 µl of primer was dispensed into the wells. Then a master mix containing 5 µl ChamQ, 1 µl cDNA and 1 µl nuclease free H_2O for each well was added for a total of 10 µl per well. After closing the plate with sealing tape it was briefly centrifuged for 30 seconds at 400 rpm to get rid of any air bubbles at the bottom. The run method was identical to that used in the primer efficiency experiments. (Table 4)

If the standard deviation of the mean Ct-values exceeded 0,3 or if one or both Ct-values of a sample were undetermined, the qPCR for the respective sample and housekeeping genes was repeated.

11.5 Statistical analysis

Data of gene expression was analyzed with GraphPad Prism 8.0.1. Relative mRNA was calculated with the 2^-delta Ct method. Outliers were identified with Grubbs' Test and removed from analysis. One-way analysis of variance (ANOVA) with a Kruskal-Wallis test for non-parametric data and Dunn's multiple comparisons test was used. The significance level (alpha) was set to 0,05.

For BAT analysis, only *Rpl4* was used as the housekeeping gene due to inconsistent gene expression of *Tbp* across the groups. For SkM analysis, both *Rpl4* and *Tbp* were employed as housekeeping genes.

12. Results

12.1 Primer efficiency test

Primer efficiency was calculated as described in 11.2. Primers were accepted when their efficiency ranged between 90% and 110%. Chosen primer pairs for the measuring of gene expression are listed in Table 5.

12.2 Gel electrophoresis of primer pairs

The qPCR products generated by all primer pairs were analyzed via agarose gel electrophoresis and subsequently visualized under UV light. Primer pairs were tested in different concentrations of cDNA, ranging from V1 (highest concentration) to V10 (lowest concentration). The electrophoresis results confirmed, that all primer

pairs selected for further experiments produced single, distinct bands corresponding to the expected amplicon sizes, with no unintended products being observed.

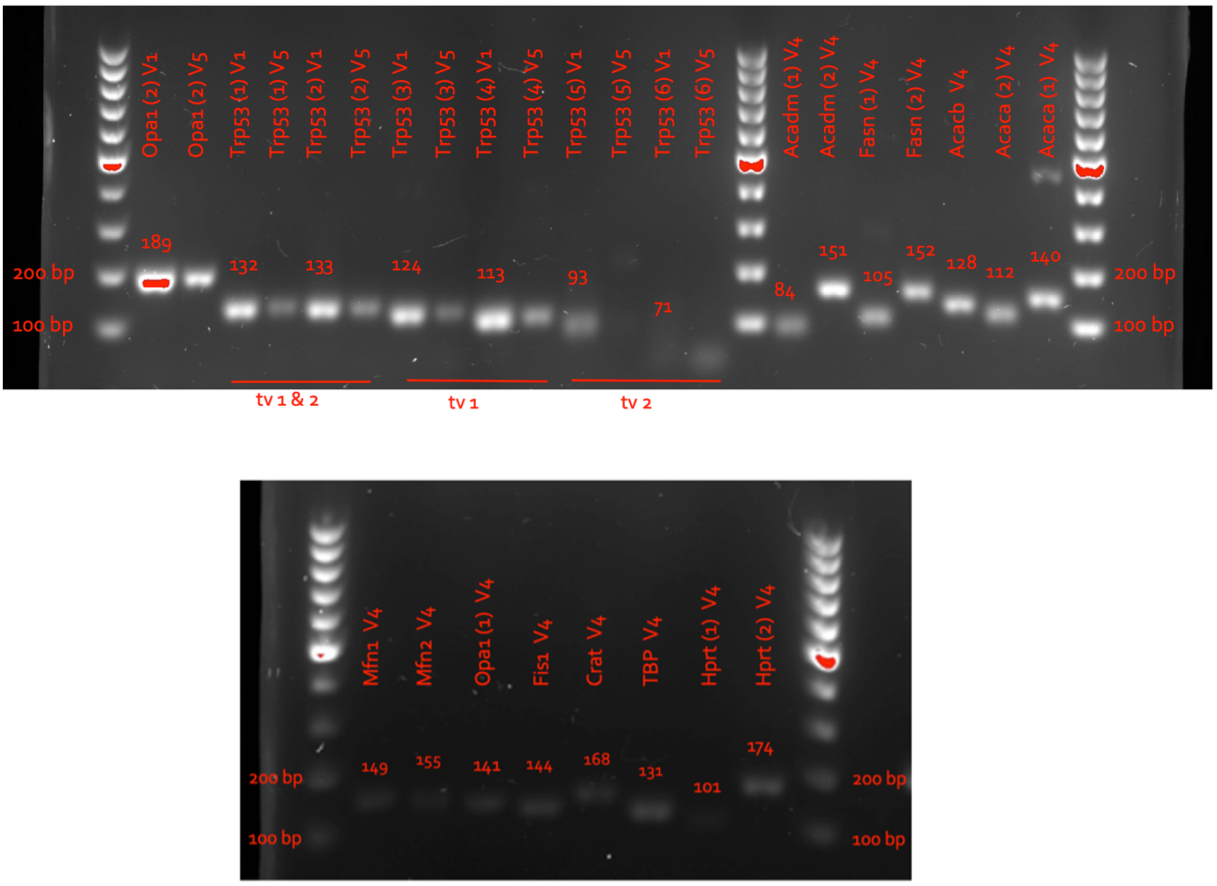

Figure 4: Gel electrophoresis of all primers, numbers over bands refer to the predicted base pair (bp) length, tv = transcript variant, V = dilution number

Table 5: Selected primer pairs used for analyzing gene expression

Primer	Direction	Sequence 5'-3'	Primer length [bp]	Amplicon length [bp]	Efficiency [%]	Company
mAcaca(2)	Forward	GCCGCCAGCCTGAGTTCTT	19	112	93,06	Microsynth
	Reverse	TGGCCAACGGAGATGGTTCA	20			
mAcacb	Forward	CTACAAGACGGCGCAGGTCA	20	128	103,49	Microsynth
	Reverse	AGGCGCCAAACTTCAGCATC	20			
mAcadm(2)	Forward	GGGGGAAAGGCCAACTGGTAT	21	151	101,18	Microsynth
	Reverse	AGCATCGCTGGCCCATGTTT	20			
mCrat	Forward	TGACTCGGCGACCTTGAACCTA	22	168	107,66	Microsynth
	Reverse	CCCAGGGGTTTTACCACGGTTC	22			
mFasn(1)	Forward	AACACGATCTGGTGCTGCCC	20	105	99,79	Microsynth
	Reverse	TGGGGGCTGTCGTGTCAGTA	20			
mFis1	Forward	GCTGGTTCTGTGTCCAAGAGCA	22	144	94,51	Microsynth

	Reverse	GACATAGTCCCGCTGTTCCTCT	22			
mHprt(1)	Forward	CAAACTTTGCTTTCCCTGGT	20	101	101,37	Microsynth
	Reverse	TCTGGCCTGTATCCAACACTTC	22			
mMfn1	Forward	CCAGGTACAGATGTCACCACAG	22	149	101,35	Microsynth
	Reverse	TTGGAGAGCCGCTCATTCACCT	22			
mMfn2	Forward	TCCCTCTGACACCTGCCAAC	20	155	90,94	Microsynth
	Reverse	TGCCTTCCACACCACTCCTC	20			
mOpa1(1)	Forward	TCCACCACAGGAAGCTCAAGAAATC	25	141	102,34	Microsynth
	Reverse	TTTTCCCAGCACTCTGATCTCCAAC	25			
mRpl4	Forward	GTATGGCACTTGGCGGAAGG	20	124	91,57	Microsynth
	Reverse	TGCTCGGAGGGCTCTTTGG	19			
mTbp	Forward	CTACCGTGAATCTTGGCTGTAAAC	24	131	102,36	Microsynth
	Reverse	AATCAACGCAGTTGTCCGTGGC	22			
mTrp53(3)	Forward	GCAGGGCTCACTCCAGCTAC	20	124	100,23	Microsynth
	Reverse	GTGATGGGGACGGGATGCAG	20			
mTrp53(5)	Forward	TTCCGGGAGCTGAATGAGGC	20	93	96,3	Microsynth
	Reverse	TCTAGGCTGGAGGCTGGAGTG	21			

12.3 Brown adipose tissue gene expression results

The mice were housed at an ambient temperature of 23°C, which is below their thermoneutral zone. As a result, they were subjected to mild cold stress, leading to continuous activation of BAT to maintain body temperature through non-shivering thermogenesis. Prolonged activation of BAT not only increases metabolic rate but also alters systemic energy balance, substrate utilization, and possibly gene expression. Warm temperatures can affect lipolysis and mouse behavior. (Farooqi & Xu, 2024) Nonetheless this setting may mimic the situation in humans well. (Speakman & Keijer, 2012).

12.3.1 LCT/MCT feeding significantly elevated Acadm expression in BAT

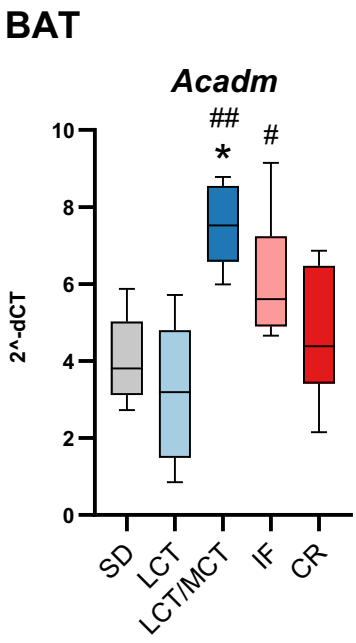

*Figure 5: Relative mRNA levels of acyl-Coenzyme A dehydrogenase, medium chain (Acadm) in brown adipose tissue (BAT) of mice fed SD, LCT, LCT/MCT, IF, CR diets after eight weeks. *P < 0.05, **P < 0.01, ***P < 0.001 vs. SD, # vs. LCT, o vs. LCT/MCT, ^ vs. IF. Statistical significance was assessed using nonparametric Kruskal-Wallis test, n = 7-8 individual mice/group. Standard diet (SD), Long-chain triglycerides (LCT), Medium-chain triglycerides (MCT), Intermittent fasting (IF), Caloric restriction (CR).*

Acadm expression was assessed to evaluate MCFA arrival and breakdown in mitochondria. In BAT, relative mRNA levels were significantly upregulated in the LCT/MCT group compared to the SD and the LCT groups. Additionally, the IF group exhibited significantly higher expression compared with the LCT group.

12.3.2 LCT feeding significantly reduced Acaca and Acacb expression in BAT

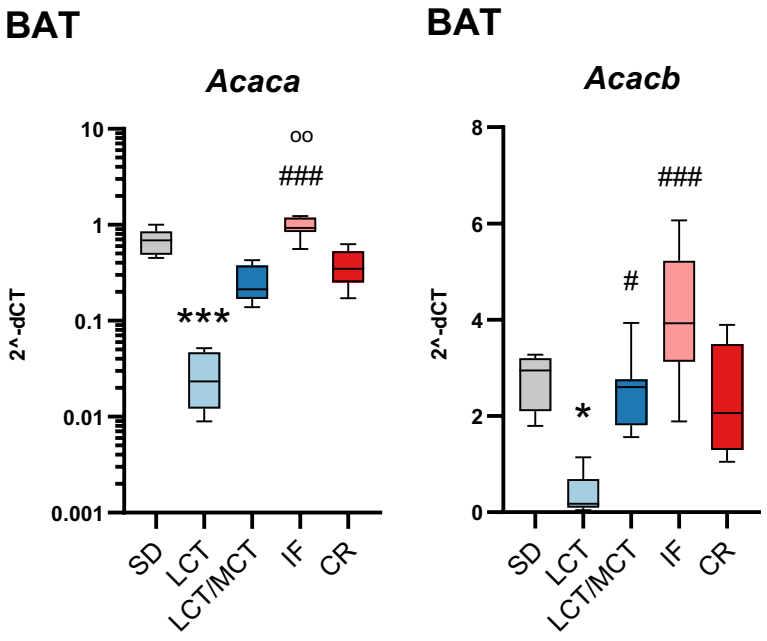

*Figure 6: Relative mRNA levels of acetyl-Coenzyme A carboxylase alpha (Acaca) and acetyl-Coenzyme A carboxylase beta (Acacb) in brown adipose tissue (BAT) of mice fed SD, LCT, LCT/MCT, IF, CR diets after eight weeks. *P < 0.05, **P < 0.01, ***P < 0.001 vs. SD, # vs. LCT, o vs. LCT/MCT, ^ vs. IF. Statistical significance was assessed using nonparametric Kruskal-Wallis test, n = 7-8 individual mice/group. Standard diet (SD), Long-chain triglycerides (LCT), Medium-chain triglycerides (MCT), Intermittent fasting (IF), Caloric restriction (CR).*

Gene expression of *Acaca* and *Acacb* was analyzed to investigate potential alterations in FAS and mitochondrial FA uptake. In BAT, the gene expression profiles of *Acaca* and *Acacb* showed similar patterns. Relative mRNA levels of both genes were significantly lower in mice fed the LCT diet compared to the SD control and IF. Additionally, *Acaca* expression was lower in the LCT/MCT group relative to the IF group, and *Acacb* expression was significantly lower in the LCT group compared with the LCT/MCT group. The overall expression levels of *Acacb* mRNA were higher than those of *Acaca*.

12.3.3 LCT and LCT/MCT feeding significantly reduced Fasn expression in BAT

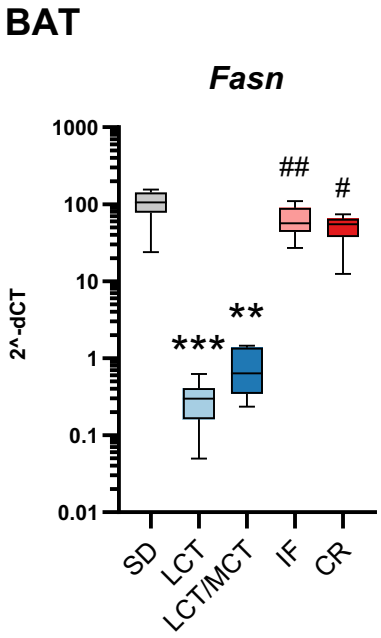

*Figure 7: Relative mRNA levels of fatty acid synthase (Fasn) in brown adipose tissue (BAT) of mice fed SD, LCT, LCT/MCT, IF, CR diets after eight weeks. *P < 0.05, **P < 0.01, ***P < 0.001 vs. SD, # vs. LCT, o vs. LCT/MCT, ^ vs. IF. Statistical significance was assessed using nonparametric Kruskal-Wallis test, n = 7-8 individual mice/group. Standard diet (SD), Long-chain triglycerides (LCT), Medium-chain triglycerides (MCT), Intermittent fasting (IF), Caloric restriction (CR).*

Fasn gene expression was assessed to evaluate *de novo* FAS in cells. In BAT, relative mRNA expression of *Fasn* was significantly downregulated in mice fed the LCT and LCT/MCT diet compared to SD control. Additionally, expression in the LCT group was significantly lower relative to IF and CR.

12.3.4 LCT and CR feeding significantly reduced Crat expression in BAT

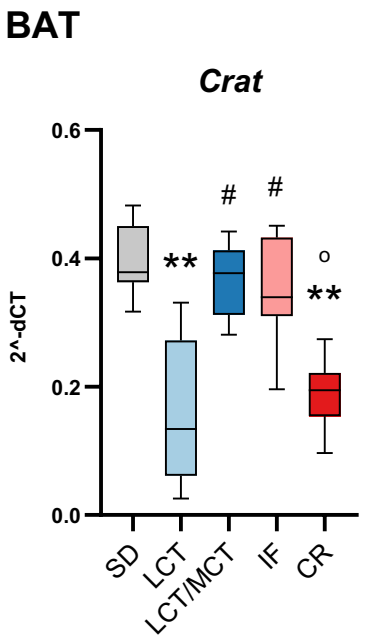

*Figure 8: Relative mRNA levels of carnitine acetyltransferase (Crat) in brown adipose tissue (BAT) of mice fed SD, LCT, LCT/MCT, IF, CR diets after eight weeks. *P < 0.05, **P < 0.01, ***P < 0.001 vs. SD, # vs. LCT, o vs. LCT/MCT, ^ vs. IF. Statistical significance was assessed using nonparametric Kruskal-Wallis test, n = 7-8 individual mice/group. Standard diet (SD), Long-chain triglycerides (LCT), Medium-chain triglycerides (MCT), Intermittent fasting (IF), Caloric restriction (CR).*

To investigate the regulation of acetyl-CoA and acetylcarnitine in mitochondria, *Crat* gene expression was analyzed. In BAT, relative mRNA expression of *Crat* was significantly lower in the LCT group relative to SD, LCT/MCT and IF. Additionally, *Crat* expression was significantly lower in the CR group compared to SD and LCT/MCT.

12.3.5 LCT/MCT feeding significantly elevated Fis1 expression in BAT

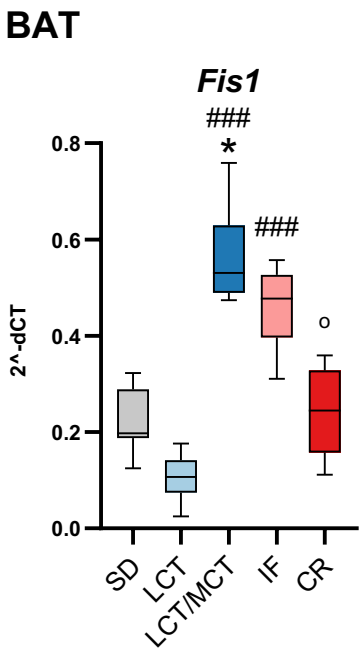

*Figure 9: Relative mRNA levels of fission, mitochondrial 1 (Fis1) in brown adipose tissue (BAT) of mice fed SD, LCT, LCT/MCT, IF, CR diets after eight weeks. *P < 0.05, **P < 0.01, ***P < 0.001 vs. SD, # vs. LCT, o vs. LCT/MCT, ^ vs. IF. Statistical significance was assessed using nonparametric Kruskal-Wallis test, n = 7-8 individual mice/group. Standard diet (SD), Long-chain triglycerides (LCT), Medium-chain triglycerides (MCT), Intermittent fasting (IF), Caloric restriction (CR).*

Fis1 gene expression was analyzed as an indicator for mitochondrial peripheral fission mechanics. In BAT, relative mRNA levels of *Fis1* were significantly elevated in mice fed the LCT/MCT diet relative to the SD, LCT and CR groups. Additionally, expression in the IF group was significantly higher than in the LCT group.

12.3.6 Mitochondrial fusion-related gene expression in BAT was not altered under ketogenic diets

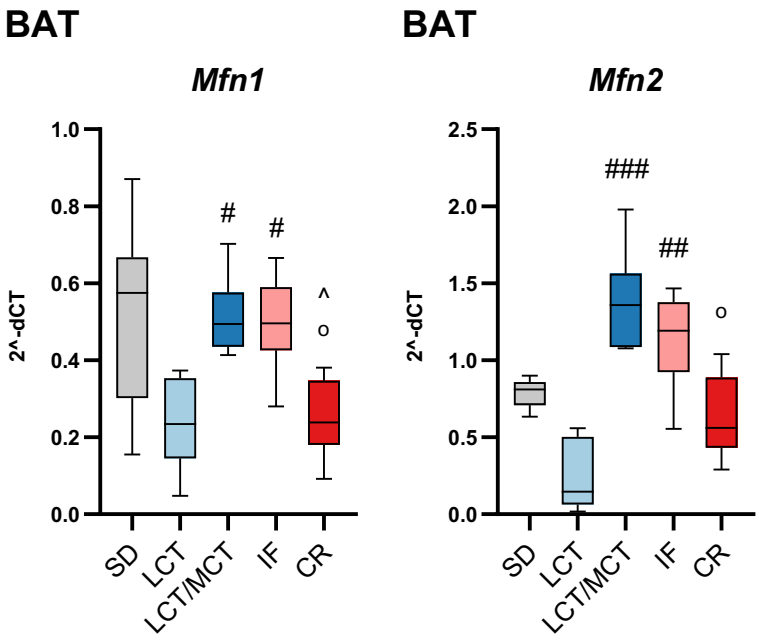

*Figure 10: Relative mRNA levels of mitofusin 1 (Mfn1) and mitofusin 2 (Mfn2) in brown adipose tissue (BAT) of mice fed SD, LCT, LCT/MCT, IF, CR diets after eight weeks. *P < 0.05, **P < 0.01, ***P < 0.001 vs. SD, # vs. LCT, o vs. LCT/MCT, ^ vs. IF. Statistical significance was assessed using nonparametric Kruskal-Wallis test, n = 7-8 individual mice/group. Standard diet (SD), Long-chain triglycerides (LCT), Medium-chain triglycerides (MCT), Intermittent fasting (IF), Caloric restriction (CR).*

Mfn1 and *Mfn2* gene expression was assessed to evaluate transcriptional drivers of mitochondrial fusion dynamics. In BAT, both genes exhibited similar regulatory patterns, with no significant differences detected relative to the SD control diet. However, gene expression levels were significantly higher in the LCT/MCT and IF groups compared to the LCT group. Additionally, the expression in the LCT/MCT group was significantly increased relative to the CR group. Furthermore, *Mfn1* expression was significantly elevated by the IF diet compared to CR.

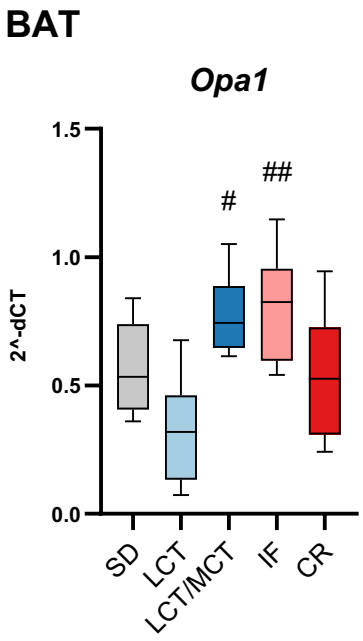

*Figure 11: Relative mRNA levels of OPA1, mitochondrial dynamin like GTPase (Opa1) in brown adipose tissue (BAT) of mice fed SD, LCT, LCT/MCT, IF, CR diets after eight weeks. *P < 0.05, **P < 0.01, ***P < 0.001 vs. SD, # vs. LCT, o vs. LCT/MCT, ^ vs. IF. Statistical significance was assessed using nonparametric Kruskal-Wallis test, n = 7-8 individual mice/group. Standard diet (SD), Long-chain triglycerides (LCT), Medium-chain triglycerides (MCT), Intermittent fasting (IF), Caloric restriction (CR).*

Opa1 expression in BAT was examined as an additional marker of mitochondrial fusion. Consistent with the *Mfn1* and *Mfn2* results, the KDs did not significantly alter gene expression relative to the SD, but relative *Opa1* mRNA levels were significantly elevated in the LCT/MCT and IF groups compared with the LCT group.

12.3.7 LCT/MCT feeding significantly elevated the expression of the longer Trp53 (l) transcript variant, and LCT and CR feeding significantly elevated the expression of the shorter Trp53 (s) transcript variant in BAT

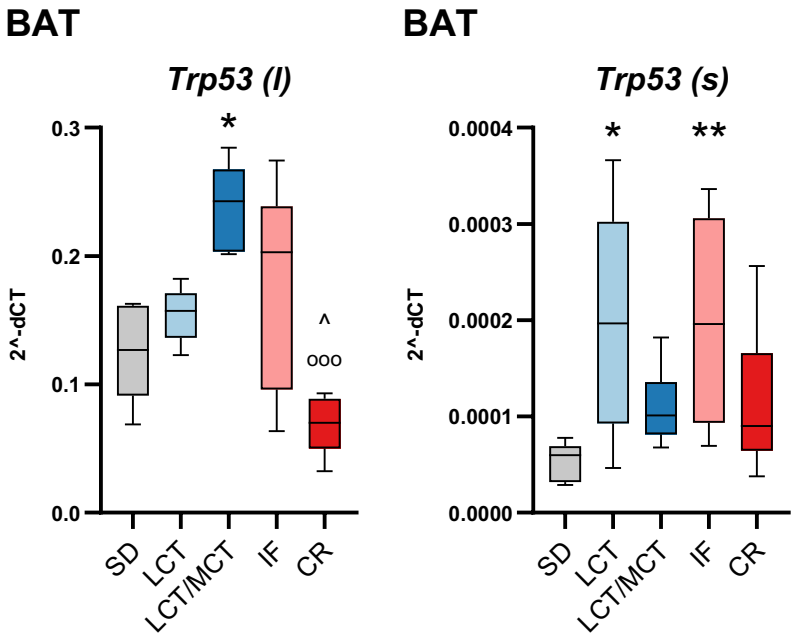

*Figure 12: Relative mRNA levels of transformation related protein 53 (Trp53) long (l) and short (s) isoform in brown adipose tissue (BAT) of mice fed SD, LCT, LCT/MCT, IF, CR diets after eight weeks. *P < 0.05, **P < 0.01, ***P < 0.001 vs. SD, # vs. LCT, o vs. LCT/MCT, ^ vs. IF. Statistical significance was assessed using non-parametric Kruskal-Wallis test, n = 7-8 individual mice/group. Standard diet (SD), Long-chain triglycerides (LCT), Medium-chain triglycerides (MCT), Intermittent fasting (IF), Caloric restriction (CR).*

Trp53 gene expression in BAT was analyzed to investigate potential differences in the activation of stress- or nutrient-related signaling pathways. The expression patterns of the two transcript variants across the groups differed in BAT. The longer variant Trp53 (l) showed significantly higher mRNA levels in the LCT/MCT group compared with SD and CR. The expression is also lowered in the CR diet compared with IF. In contrast, the shorter variant Trp53 (s) was significantly elevated in the LCT and IF groups compared with SD. Furthermore, Trp53 (s) is expressed at markedly lower levels, approximately 1/1000 of those observed for Trp53 (l).

12.4 Skeletal muscle tissue gene expression results

Overall in SkM, the observed effects of the KDs on gene expression were not as pronounced as those observed in BAT, indicating that SkM may be less sensitive to dietary induced changes.

12.4.1 LCT/MCT feeding significantly elevated Acadm expression in SkM

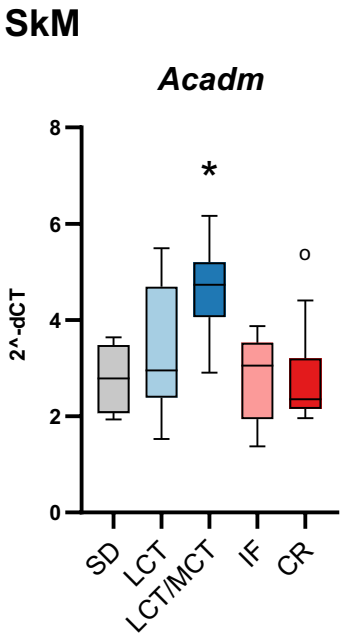

*Figure 13: Relative mRNA levels of acyl-Coenzyme A dehydrogenase, medium chain (Acadm) in skeletal muscle tissue (SkM) of mice fed SD, LCT, LCT/MCT, IF, CR diets after eight weeks. *P < 0.05, **P < 0.01, ***P < 0.001 vs. SD, # vs. LCT, o vs. LCT/MCT, ^ vs. IF. Statistical significance was assessed using nonparametric Kruskal-Wallis test, n = 6-8 individual mice/group. Standard diet (SD), Long-chain triglycerides (LCT), Medium-chain triglycerides (MCT), Intermittent fasting (IF), Caloric restriction (CR).*

Similar to BAT, relative mRNA levels were significantly higher in the LCT/MCT group compared with the SD control and CR group.

12.4.2 LCT/MCT feeding significantly elevated Acaca and Acacb expression in SkM

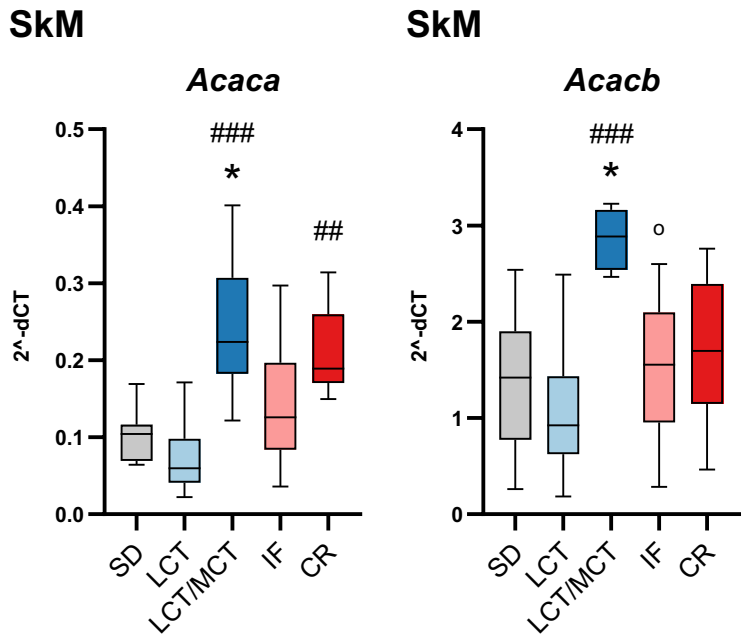

*Figure 14: Relative mRNA levels of acetyl-Coenzyme A carboxylase alpha (Acaca) and acetyl-Coenzyme A carboxylase beta (Acacb) in skeletal muscle tissue (SkM) of mice fed SD, LCT, LCT/MCT, IF, CR diets after eight weeks. *P < 0.05, **P < 0.01, ***P < 0.001 vs. SD, # vs. LCT, o vs. LCT/MCT, ^ vs. IF. Statistical significance was assessed using nonparametric Kruskal-Wallis test, n = 6-8 individual mice/group. Standard diet (SD), Long-chain triglycerides (LCT), Medium-chain triglycerides (MCT), Intermittent fasting (IF), Caloric restriction (CR).*

As observed in BAT, both genes displayed similar expression patterns between each other, although the overall trends differed from those in BAT. The LCT/MCT group exhibited significantly higher relative mRNA expression of both *Acaca* and *Acacb* compared with the SD and LCT groups. Additionally, *Acacb* expression in the LCT/MCT group was significantly higher than in IF, and *Acaca* expression was significantly higher in the CR compared to the LCT group. Similar to BAT, the overall *Acacb* expression was generally higher than that of *Acaca* in SkM.

12.4.3 Fasn expression remained stable in SkM under ketogenic diets

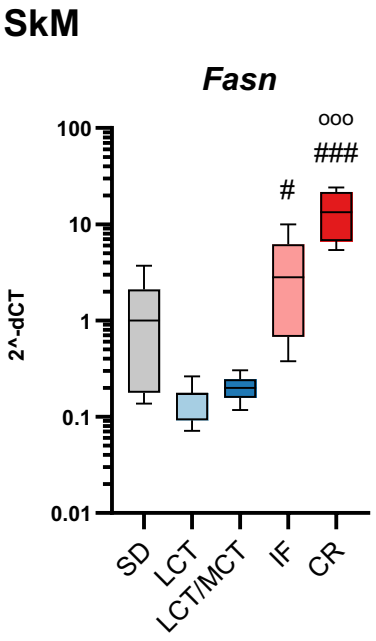

*Figure 15: Relative mRNA levels of fatty acid synthase (Fasn) in skeletal muscle tissue (SkM)) of mice fed SD, LCT, LCT/MCT, IF, CR diets after eight weeks. *P < 0.05, **P < 0.01, ***P < 0.001 vs. SD, # vs. LCT, o vs. LCT/MCT, ^ vs. IF. Statistical significance was assessed using nonparametric Kruskal-Wallis test, n = 6-8 individual mice/group. Standard diet (SD), Long-chain triglycerides (LCT), Medium-chain triglycerides (MCT), Intermittent fasting (IF), Caloric restriction (CR).*

The relative mRNA expression levels in SkM were significantly elevated in the IF and CR groups compared with the LCT group, and significantly elevated in the CR group compared with the LCT/MCT group. In contrast to BAT, no significant differences were observed between the LCT, LCT/MCT and SD groups in SkM.

12.4.4 Crat expression remained stable in SkM under ketogenic diets

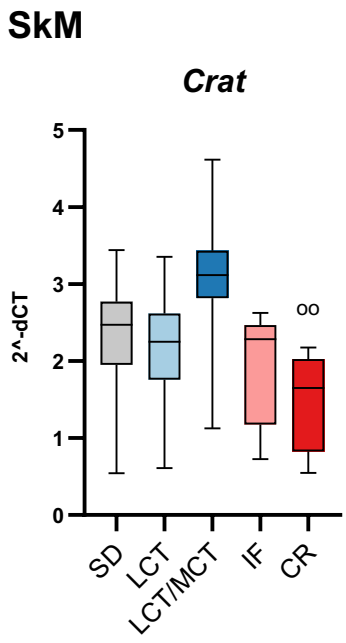

*Figure 16: Relative mRNA levels of carnitine acetyltransferase (Crat) in skeletal muscle tissue (SkM) of mice fed SD, LCT, LCT/MCT, IF, CR diets after eight weeks. *P < 0.05, **P < 0.01, ***P < 0.001 vs. SD, # vs. LCT, o vs. LCT/MCT, ^ vs. IF. Statistical significance was assessed using nonparametric Kruskal-Wallis test, n = 6-8 individual mice/group. Standard diet (SD), Long-chain triglycerides (LCT), Medium-chain triglycerides (MCT), Intermittent fasting (IF), Caloric restriction (CR).*

Crat relative mRNA expression in SkM was significantly higher in the LCT/MCT group compared to CR, with no significant differences observed between the other groups.

12.4.5 Fis1 expression remained stable in SkM under ketogenic diets

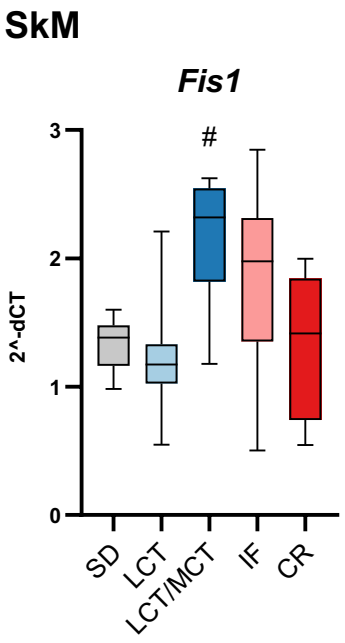

*Figure 17: Relative mRNA levels of fission, mitochondrial 1 (Fis1) in skeletal muscle tissue (SkM) of mice fed SD, LCT, LCT/MCT, IF, CR diets after eight weeks. *P < 0.05, **P < 0.01, ***P < 0.001 vs. SD, # vs. LCT, o vs. LCT/MCT, ^ vs. IF. Statistical significance was assessed using nonparametric Kruskal-Wallis test, n = 6-8 individual mice/group. Standard diet (SD), Long-chain triglycerides (LCT), Medium-chain triglycerides (MCT), Intermittent fasting (IF), Caloric restriction (CR).*

Fis1 relative mRNA expression in SkM was significantly higher in mice fed the LCT/MCT diet compared to the LCT diet. In contrast to BAT, no significant differences were observed between the other groups.

12.4.6 Mitochondrial fusion-related gene expression in SkM was not altered under ketogenic diets

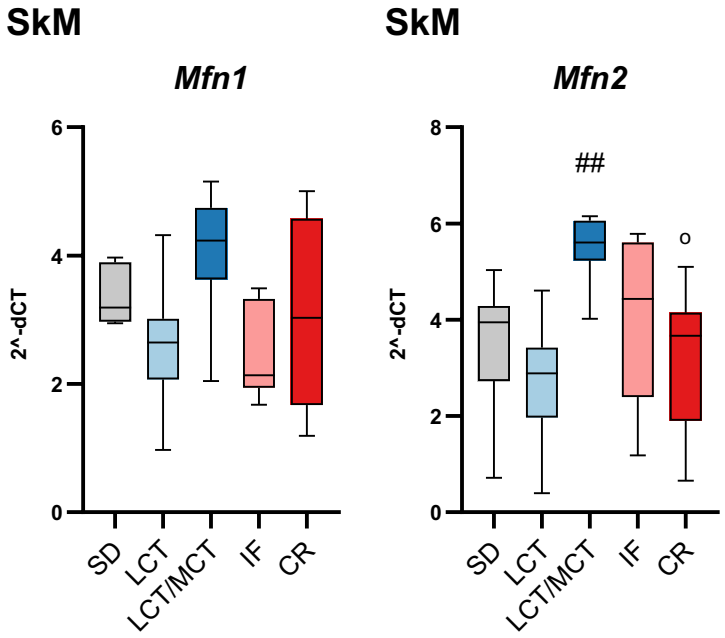

*Figure 18: Relative mRNA levels of mitofusin 1 (Mfn1) and mitofusin 2 (Mfn2) in skeletal muscle tissue (SkM) of mice fed SD, LCT, LCT/MCT, IF, CR diets after eight weeks. *P < 0.05, **P < 0.01, ***P < 0.001 vs. SD, # vs. LCT, o vs. LCT/MCT, ^ vs. IF. Statistical significance was assessed using nonparametric Kruskal-Wallis test, n = 6-8 individual mice/group. Standard diet (SD), Long-chain triglycerides (LCT), Medium-chain triglycerides (MCT), Intermittent fasting (IF), Caloric restriction (CR).*

In SkM, the relative mRNA expression levels of *Mfn1* in SkM showed no significant differences between groups, whereas *Mfn2* expression was significantly upregulated in the LCT/MCT group in comparison to the LCT and CR groups.

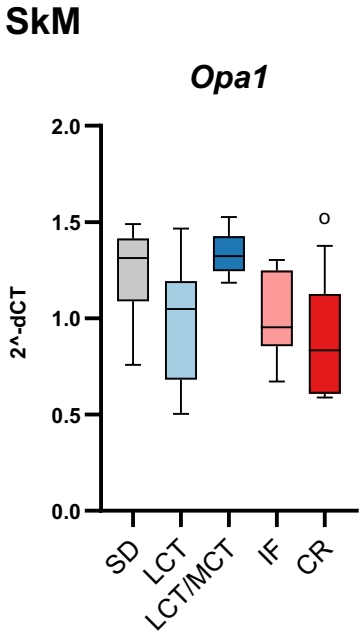

*Figure 19: Relative mRNA levels of OPA1, mitochondrial dynamin like GTPase (Opa1) in skeletal muscle tissue (SkM) of mice fed SD, LCT, LCT/MCT, IF, CR diets after eight weeks. *P < 0.05, **P < 0.01, ***P < 0.001 vs. SD, # vs. LCT, o vs. LCT/MCT, ^ vs. IF. Statistical significance was assessed using nonparametric Kruskal-Wallis test, n = 6-8 individual mice/group. Standard diet (SD), Long-chain triglycerides (LCT), Medium-chain triglycerides (MCT), Intermittent fasting (IF), Caloric restriction (CR).*

The relative gene expression levels of *Opa1* were significantly lower in mice fed the CR diet than in mice fed the LCT/MCT diet, with no significant differences observed between the other groups.

12.4.7 LCT feeding significantly elevated the expression of the shorter Trp53 (s) transcript variant in SkM

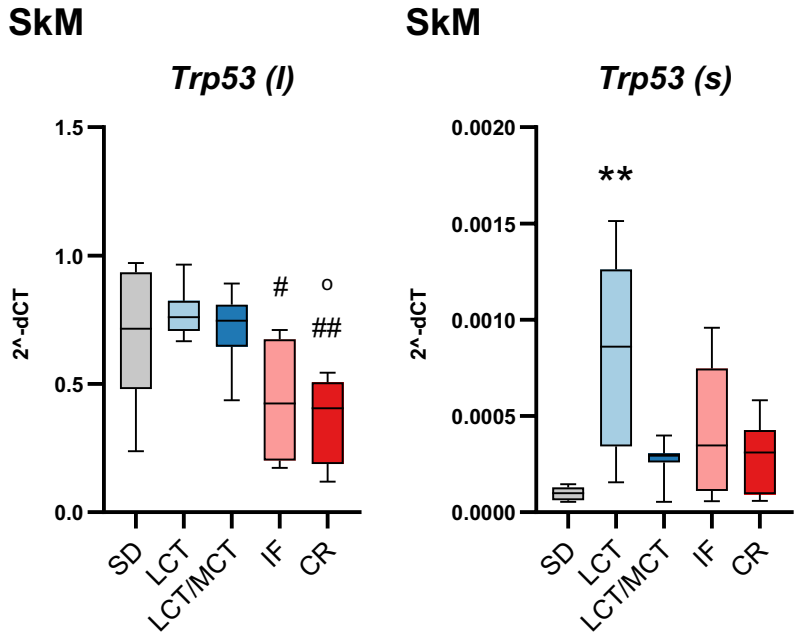

*Figure 20: Relative mRNA levels of transformation related protein 53 (Trp53) long (l) and short (s) isoform in skeletal muscle tissue (SkM) of mice fed SD, LCT, LCT/MCT, IF, CR diets after eight weeks. *P < 0.05, **P < 0.01, ***P < 0.001 vs. SD, # vs. LCT, o vs. LCT/MCT, ^ vs. IF. Statistical significance was assessed using non-parametric Kruskal-Wallis test, n = 7-8 individual mice/group. Standard diet (SD), Long-chain triglycerides (LCT), Medium-chain triglycerides (MCT), Intermittent fasting (IF), Caloric restriction (CR).*

Similar to BAT, the expression patterns of the Trp53 (l) and Trp53 (s) transcript variants between them also differed in SkM. Relative mRNA levels of Trp53 (l) were significantly reduced in the IF and CR groups compared to LCT, with CR also showing reduced expression compared to LCT/MCT. In contrast and similar to BAT, Trp53 (s) was significantly upregulated in the LCT group compared to SD. As observed in BAT, expression of the longer variant is approximately 1000 times higher than that of the shorter variant.

13. Discussion

Feeding mice an MCT-heavy KD induced pronounced transcriptional responses across multiple genes related to FA metabolism in both BAT and SkM in previous studies by Sternberg et al. (2025, unpublished data). (Supplementary Figure 1) Consistent with these findings, this study demonstrates that the LCT/MCT KD elicits transcriptional changes, supporting the hypothesis that MCTs induce a distinct metabolic stimulus beyond that of a classic LCT-KD.

This discussion will primarily address the changes induced by the LCT/MCT feeding, as covering all dietary groups in detail would exceed the scope of this thesis. When interpreting the gene expression results, it must be taken into account that only *Rpl4* was used as the housekeeping gene for BAT, whereas both *Rpl4* and *Tbp* were employed for SkM. Consequently, a direct comparison of expression levels between tissues is not possible.

13.1 Ketone bodies serve as an alternative energy source in SkM on a KD

To determine whether KDs increased KB production and whether KBs might mediate the observed metabolic effects, β-OHB levels were analyzed. Only in SkM did the KDs raise β-OHB levels (Supplementary Figure 4), indicating that mice fed a KD, whether supplemented with MCTs or containing mainly LCTs, produced significantly more KBs which were utilized by SkM as an energy source.

In contrast, BAT showed no accumulation of β-OHB in mice fed a KD, suggesting a predominant reliance on other substrates, such as LCFAs, that serve as fuels for thermogenesis. Alternatively, BAT may have maintained a high rate of KB oxidation, preventing detectable accumulation. These results suggest tissue specific differences in KB metabolism between BAT and SkM.

13.2 Medium- and long-chain fatty acid oxidation

To determine whether MCFAs effectively reached peripheral tissues and were metabolized there, the expression of *Acadm* was analyzed. As expected, the LCT/MCT feeding markedly increased *Acadm* expression in both BAT and SkM, indicating enhanced MCFA oxidation. This upregulation was absent with the LCT feeding, suggesting that the observed effect is caused by the MCTs in the diet. Consistent with these finding, lipid analyses revealed elevated tissue levels of C8:0 and C10:0 following LCT/MCT feeding, supporting the notion that these FAs were not fully oxidized in the liver but instead reached extrahepatic tissues, where they could be rapidly metabolized. (Supplementary Figure 3)

In contrast, *Acadm* expression remained unchanged in the LCT-fed mice, despite a comparable FA load to that in the LCT/MCT diet. This was unexpected, as a higher supply with LCFA would be expected to increase MCAD activity to support increased FAO. One possible explanation is that the activity of other acyl-CoA dehydrogenase isozymes is sufficient to accommodate the increased LCFA load, thereby eliminating the need for upregulation of *Acadm* expression in BAT. Alternatively, excess FAs may have been stored as TGs in adipose tissue, which is supported by the observed increase of relative epididymal WAT (eWAT) in the LCT-fed mice. (Supplementary Figure 2)

Interestingly, lipid profiling further revealed distinct tissue-specific differences. C10:0 was significantly elevated in both BAT and SkM of LCT/MCT-fed mice, whereas C8:0 accumulation was observed only in SkM. This suggests that BAT preferentially oxidizes LCFAs, while SkM relies more on MCFAs and KBs as rapid energy substrates. Alternatively, BAT oxidizes C8:0 so efficiently that no accumulation was detected. (Supplementary Figure 3)

Given that C10:0 is metabolized differently than C8:0 and more similarly to LCFAs (Khabbush et al., 2017), its accumulation may indicate a greater dependence on carnitine-mediated transport. Consistent with this, C8:0- and C10:0-carnitines were detected in both tissues, with SkM showing significant increases under the LCT/MCT feeding. (Supplementary Figure 3) This implies that MCFAs partially depend on the carnitine shuttle for mitochondrial import, in line with previous reports.

(Khabbush et al., 2017) But this effect may be tissue specific, since C8:0- and C10:0-carnitines were only elevated in SkM but not in BAT. Furthermore, C8:0 and C8:0-carnitine are present at lower levels than C10:0 and C10:0-carnitine respectively, even though both FAs are present at equal amounts in the LCT/MCT diet, this suggests that C8:0 is metabolized more rapidly than C10:0, consistent with prior studies reporting faster C8:0 oxidation and that a KD and MCTs enhance oxidative metabolism in SkM. (Charlot et al., 2022; Wallace et al., 2021) Additionally, these findings align with previous reports showing that the dependence of MCFA oxidation on carnitine is tissue specific, with SkM requiring carnitine for this metabolic pathway, whereas other tissues may oxidize MCFAs more independently. (Pereyra et al., 2023)

In addition to MCFA, LCFA oxidation may also have been enhanced by the LCT/MCT diet, as genes encoding the carnitine shuttle components, *Cpt1a* and *Slc25a20* (solute carrier family 25 (mitochondrial carnitine/acylcarnitine translocase), member 20) (Supplementary Figure 1), were upregulated in both tissues. Moreover, given that MCTs are known activators of PPARs (Liberato et al., 2012), the concomitant increase in *Pparg1* and *Plin5* expression (Supplementary Figure 1) further implies, that the addition of MCTs may promote metabolic adaptations, such as enhanced FAO through activation of PGC-1α and regulation of mitochondrial oxidative capacity. (Gallardo-Montejano et al., 2016; X. Zhang et al., 2022)

13.3 Increased malonyl-CoA production in SkM by MCTs

To further investigate the FA metabolism, *Acaca* and *Acacb* gene expression was analyzed. In contrast to BAT, the LCT/MCT diet markedly upregulated both genes in SkM, suggesting potentially enhanced activity of ACCs and malonyl-CoA production, favoring the inhibition of LCFA oxidation while simultaneously promoting FAS. ACC activity is typically upregulated when there is more energy available than needed. (Wang et al., 2022) Based on this, mice fed the LCT/MCT diet may have had a relative energy surplus, thereby oxidizing fewer LCFAs and diverting more toward TG storage. However, data from Sternberg et al. (unpublished data, 2025) shows, that the LCT/MCT group did not gain relative eWAT mass, whereas the LCT group did (Supplementary Figure 2), suggesting that this potential energy surplus did not translate into enhanced lipid storage in the LCT/MCT-fed mice.

Furthermore, *Fasn* expression was unaltered by the LCT/MCT feeding in the SkM, suggesting that FASN activity, and consequently *de novo* FAS, remained unchanged. This appears contradictory, as malonyl-CoA generated by ACC1 is typically further metabolized to C16:0 by FASN and malonyl-CoA generated by ACC2 would indirectly inhibit FAO. This raises the possibility of an accumulation of malonyl-CoA, potentially leading to the inhibition of mTORC1 and subsequent attenuation of anabolic pathways. (Nicastro et al., 2023)

Alternatively, the observed *Acaca* and *Acacb* upregulation by the LCT/MCT feeding could be connected to the upregulation of *Acadm* in LCT/MCT mice, and together this may reflect a metabolic shift toward preferential MCFA oxidation. In this context, cells might actively restrict LCFA import via CPT1 to favor MCFA utilization. However, *Cpt1a* and the *Slc25a20* were significantly upregulated in the LCT/MCT fed mice as well, suggesting an overall activation of the carnitine shuttle and therefore enhanced LCFA-import into mitochondria (Supplementary Figure 1), raising the question of how genes involved in both malonyl-CoA production and carnitine shuttle function can be simultaneously upregulated by the same diet. One possible explanation is that MCFAs, such as C8:0 and C10:0, are still partially dependent on the carnitine shuttle for FAO. (Khabbush et al., 2017) This implies that that MCFAs may not bypass the carnitine shuttle entirely, contrary to the conventional view that MCFAs freely diffuse across the mitochondrial membrane. (Nimbkar et al., 2022) The absence of a similar response in LCT-fed mice further supports a unique, MCT-dependent regulatory mechanism. Taken together, these findings suggest that the upregulation of *Acaca* and *Acacb* in SkM following the LCT/MCT feeding may represent a regulatory mechanism to fine-tune and optimize mitochondrial FAO activity.

Conversely in BAT, the LCT diet significantly lowered both *Acaca* and *Acacb* expression, suggesting reduced ACC1 and ACC2 activity. This downregulation may result in the reduction of malonyl-CoA and consequently an increase of LCFA uptake into the mitochondria, while simultaneously attenuating *de novo* FAS. Consistent with this, *Fasn* expression was also decreased in the LCT group, further indicating reduced FAS in BAT by the LCT feeding. Notably, the LCT/MCT feeding did not affect *Acaca* and *Acacb* expression in BAT.

These findings suggest tissue-specific differences in how BAT and SkM adapt their FA metabolism to high-fat feeding.

13.4 Suppression of *de novo* fatty acid synthesis in BAT

The modulation of *de novo* FAS in different tissues in response to dietary interventions provides further insights into their metabolism. The observed downregulation of *Fasn* by the LCT and LCT/MCT feeding in BAT suggests a reduced *de novo* FAS in these mice. This decrease is likely due to the high availability of exogenous FAs provided by the high-fat diets, reducing the cellular demand for endogenous synthesis. This indicates that BAT under ketogenic conditions relies less on synthesis and more on dietary or stored FAs. These findings are consistent with those of Yamasaki et al. (2023), who also reported downregulation of *Acaca* and *Fasn* in BAT of mice fed a high-fat diet, as well as with Yahagi et al. (2003), who demonstrated that p53 is induced upon refeeding and negatively regulates lipogenic genes in *ob/ob* adipocytes.

In contrast, FASN levels in SkM appear unaltered across the LCT and LCT/MCT groups, suggesting that the KD interventions did not alter the rate of *de novo* FAS. Similar to BAT, this may also reflect sufficient FA availability from the diet, making the increase of endogenous synthesis redundant. However, given that SkM has a relatively low contribution to *de novo* FAS under physiological baseline conditions (Watt & Hoy, 2012), the absence of transcriptional change is not unexpected.

Interestingly, in the IF and CR groups, *Fasn* expression remained unchanged in both BAT and SkM. This finding contrasts with the expected downregulation typically associated with fasting and caloric restriction, which are known to activate AMPK and subsequently suppress *Fasn* transcription and FAS activity. The absence of this expected downregulation may indicate tissue-specific regulation or that the degree or duration of AMPK activation was not sufficient to trigger measurable transcriptional effects.

13.5 Mitochondria related gene expression in response to the LCT/MCT feeding

To assess whether elevated FA availability promotes mitochondrial fragmentation and thereby facilitates increased LCFA oxidation, *Fis1* gene expression was analyzed. In BAT, LCT/MCT feeding elevated *Fis1* expression, suggesting increased peripheral mitochondrial fission and thus the enhanced ability to import LCFAs into mitochondria and increase FAO. (Ngo et al., 2023)

In contrast, the SkM did not alter *Fis1* levels, indicating that the LCT/MCT mediated enhanced fission may be specific for BAT. BAT, which typically relies heavily on glucose oxidation (Carpentier et al., 2018), may shift its metabolism toward FAO under KD feeding, necessitating increased mitochondrial fission to accommodate elevated FA abundance. Notably, this effect was MCT specific and not observed with the LCT feeding, suggesting that MCTs play a unique role in modulating mitochondrial dynamics in BAT.

Alternatively, the upregulation of *Fis1* by the LCT/MCT feeding in BAT may reflect enhanced mitochondrial quality control mechanisms. Increased fission could serve as a mechanism to remove damaged mitochondria through mitophagy. This interpretation is supported by a possible increase of TP53 in BAT, as the increased FAO induced by the LCT/MCT-KD, may generate higher oxidative stress, leading to mitochondrial damage. In response, BAT may upregulate *Trp53* and *Fis1* to mitigate cellular stress. Increased TP53 protein levels may promote FAO and OXPHOS while suppressing FAS and glycolysis, potentially as a downstream effect of AMPK activation. (Temaj et al., 2024; S.-J. Wei et al., 2024)

To further explore potential alterations in energy metabolism and metabolic health, additional genes involved in mitochondrial dynamics were analyzed. Mitochondrial fusion seems to be unaltered by the LCT/MCT feeding in BAT. However, the LCT/MCT and IF diets increased the expression of all mitochondrial dynamics-related genes compared with the classical LCT-KD. These findings suggest that mitochondrial turnover, including mitophagy and biogenesis, may be more actively regulated by the addition of MCTs to a KD or by fasting intermittently, compared with a classic KD in BAT.

In contrast, SkM did not alter its mitochondrial dynamics-related gene expression in response to MCTs, and neither fusion nor fission seem to be altered by the LCT/MCT feeding. Since SkM inherently relies less on glucose (Carpentier et al., 2018), it may therefore not require morphological remodeling to meet energetic demands. These results highlight tissue-specific differences in the regulation of mitochondrial morphology in response to MCT-based KDs between BAT and SkM.

Prior studies have shown that MCFAs, particularly C8:0, can stimulate AMPK and PGC-1α signaling and may promote mitochondrial biogenesis and OXPHOS in SkM. (Charlot et al., 2022; Nishida et al., 2024) In this study, mitochondrial turnover may be enhanced by the LCT/MCT diet, but only compared to the LCT-KD, as *Fis1* and *Mfn2* expression was upregulated. Given the additional upregulation of *Vdac* and *Pparg1* in both tissues, this may reflect elevated PGC-1α mediated mitochondrial biogenesis in both tissues, compared with the LCT diet (Supplementary Figure 1). These findings suggest, that the LCT/MCT diet may be superior in increasing mitochondrial turnover to a classic KD by enhancing PGC-1α activity and mitochondrial biogenesis in both SkM and BAT.

Notably, mice fed an LCT-only KD gained more eWAT relative to body weight (Supplementary Figure 2), whereas LCT/MCT-fed mice did not, further suggesting that MCTs confer metabolic advantages, possibly by improving mitochondrial function.

13.6 Future perspective

As the beneficial effects of KDs, KBs and MCTs have been attracting increased scientific attention, alternatives to the highly restrictive KDs are being explored to achieve similar metabolic benefits with fewer limitations.

Exogenous ketogenic supplements, such as MCT oils (C8:0/C10:0), ketone esters and ketone salts offer alternative means to elevate KB levels without requiring strict KD adherence or fasting. (Jensen et al., 2020) Acute supplementation with ketone monoesters or salts increases blood β-OHB levels while decreasing blood glucose levels, with monoesters being markedly more effective. (Falkenhain et al., 2022) However, potential risks include hepatic lipid accumulation associated with certain MCFAs, especially C12:0 from coconut oil (Goetzman et al., 2020), and

supplementation with exogenous ketones may increase the risk of ketoacidosis, as the body's buffering capacity may be insufficient to maintain normal blood pH. (Kolb et al., 2021)

Nevertheless, the therapeutic potential of supplementation remains promising. Emerging evidence suggests potential therapeutic effects of MCT supplementation, such as enhanced cognitive performance in both healthy individuals and those with cognitive impairment. (Shcherbakova et al., 2022) A ketogenic drink elevated plasma KBs and improved cognitive outcomes in adults with mild cognitive impairment. (Fortier et al., 2021) Additional potential applications of MCT supplementation include the enhancement of endurance performance, treating muscle dysfunction and to support weight management. In contrast to nutritional ketosis, exogenous KB administration induces an "artificial" metabolic state that may hold therapeutic promise for conditions such as heart diseases. (Kolb et al., 2021) Additionally, certain pharmacological interventions such as SGLT2 inhibitors, commonly prescribed for the treatment of type 2 diabetes mellitus, can elevate circulating KB levels, further highlighting the clinical relevance of ketone metabolism. (Kolb et al., 2021)

It remains to be determined whether MCT supplementation alone, without carbohydrate restriction, could provide measurable benefits. In humans, the dietary carbohydrate content may not influence MCT absorption, but the KB production rate. (St-Pierre et al., 2019) Furthermore, it remains to be clarified to what extent MCT or KB supplements can exert beneficial effects independently of ketosis. Moreover, the precise mechanisms and long-term effects by which MCTs and KBs influence cognition and metabolic health remain to be fully elucidated.

Further studies should explore whether combining the MCT-based KD with CR or IF could enhance ketogenic and longevity-associated effects. The interplay between MCFAs, LCFAs and mitochondrial morphology warrants further investigation, particularly under physiological stress conditions such as exercise or cold exposure. Future research should aim to expand current findings by including a broader set of gene expression analyses, validating at the protein level and performing long-term human studies.

13.7 Limitations

This study is limited to the investigation of intracellular mechanisms and does not account for the broader network of intercellular and systemic signaling pathways that may also influence the observed outcomes. While this focused approach provides valuable mechanistic insight, it does not capture the full physiological complexity, including hormonal, neural, or immune-mediated regulatory inputs that could modulate metabolism *in vivo*. Additionally, because of mRNA degradation and post-transcriptional modifications, mRNA data cannot be considered alone, because it may not always correlate directly with the protein activity.

14. Zusammenfassung

Fettsäuren spielen eine wesentliche Rolle in der menschlichen Ernährung, da sie sowohl als Energiequelle als auch als strukturelle Bestandteile von Zellen dienen. Ketogene Diäten (KD), bei denen Fette den Großteil der Energieaufnahme darstellen, werden seit 100 Jahren zur Behandlung von Epilepsie bei Kindern eingesetzt. In den letzten Jahren gewinnt ihr Einsatz auch für andere Krankheitsbilder zunehmend an Bedeutung, darunter neurodegenerative und metabolische Erkrankungen.

Um den Einfluss verschiedener Ernährungsinterventionen auf den Stoffwechsel zu untersuchen, wurde braunes Fettgewebe (BAT) und Skelettmuskel (SkM) von Mäusen analysiert, welche entweder mit einer Standarddiät (SD), einer KD mit hauptsächlich langkettigen Triglyzeriden (LCT), einer KD mit einem 70/30 Verhältnis von LCT zu mittelkettigen Fettsäuren (LCT/MCT), einer intermittierenden Fasten Diät (IF) oder einer kalorienreduzierten Diät (CR) gefüttert wurden. Vorherige Studien von Sternberg et al. (2025, unveröffentlichte Daten) zeigten, dass die LCT/MCT-Diät transkriptionelle Veränderungen in Verbindung mit dem Fettstoffwechsel in sowohl SkM als auch BAT auslöste. Aufbauend auf diesen Ergebnissen untersucht die vorliegende Arbeit die Expression ausgewählter Gene in diesen Geweben mit quantitativer Echtzeit-PCR, um tiefere Einblicke in die molekularen Mechanismen zu gewinnen über die unterschiedlichen Arten von Fetten den Stoffwechsel und mitochondriale Funktionen beeinflussen.

Die LCT/MCT Ernährung führte zu signifikanten Veränderungen der Genexpression in sowohl BAT als auch SkM. Während in beiden Geweben vermutlich eine verstärkte Fettsäureoxidation stattfand, scheint BAT seinen Stoffwechsel von der Fettsäuresynthese in Richtung Fettsäureoxidation gerichtet zu haben, wohingegen SkM möglicherweise die Oxidation langkettiger Fettsäuren einschränkte. Darüber hinaus zeigten sich im BAT transkriptionelle Veränderungen die auf eine verstärkte mitochondriale Fission sowie auf erhöhten oxidativen Stress hindeuten.

15. Abbreviations

BAT	Brown adipose tissue
Acaca	acetyl-Coenzyme A carboxylase alpha
Acacb	acetyl-Coenzyme A carboxylase beta
Acadm	acyl-Coenzyme A dehydrogenase, medium chain
ACC	acetyl-Coenzyme A carboxylase
ACC1	acetyl-Coenzyme A carboxylase alpha
ACC2	acetyl-Coenzyme A carboxylase beta
C8:0	caprylic acid
C10:0	capric acid
C12:0	lauric acid
C16:0	palmitic acid
CACT	carnitine-acylcarnitine translocase
CoA	Coenzyme A
CPT1	carnitine palmitoyltransferase 1
Cpt1a	carnitine palmitoyltransferase 1a, liver
CR	Caloric restriction
Crat	carnitine acetyltransferase
CRAT	carnitine O-acetyltransferase
FA	Fatty acid
FAO	Fatty acid oxidation
FAS	Fatty acid synthesis
Fasn/FASN	fatty acid synthase
Fis1	fission, mitochondrial 1
FIS1	mitochondrial fission 1 protein
IF	Intermittent fasting
IMM	Inner mitochondrial membrane
KB	Ketone body
KD	Ketogenic diet
LCFA	Long chain fatty acid
LCT	Long chain triglyceride
MCFA	Medium chain fatty acid
MCT	Medium chain triglyceride
Mfn1/MFN1	mitofusin 1
Mfn2/MFN2	mitofusin 2
OMM	Outer mitochondrial membrane
Opa1	OPA1, mitochondrial dynamin like GTPase
OPA1	optic atrophy protein 1
OXPHOS	Oxidative phosphorylation

p53	tumor suppressor p53
Plin5/PLIN5	perilipin 5
Pparg1	peroxisome proliferator activated receptor gamma transcript variant 1
PPARgamma	peroxisome proliferator-activated receptor gamma
ROS	Reactive oxigen species
Rpl4	ribosomal protein L4
Slc25a20	solute carrier family 25 (mitochondrial carnitine/acylcarnitine translocase), member 20
SD	Standard diet
SkM	Skeletal muscle
Tbp	TATA box binding protein
Trp53 (l)	transformation related protein 53 long transcript variant
Trp53 (s)	transformation related protein 53 short transcript variant
Vdac/VDAC	voltage-dependent anion channel

16. References

Abu-Elheiga, L., Matzuk, M. M., Abo-Hashema, K. A. H., & Wakil, S. J. (2001). Continuous Fatty Acid Oxidation and Reduced Fat Storage in Mice Lacking Acetyl-CoA Carboxylase 2. *Science*, *291*(5513), 2613–2616. https://doi.org/10.1126/science.1056843

Abu-Elheiga, L., Matzuk, M. M., Kordari, P., Oh, W., Shaikenov, T., Gu, Z., & Wakil, S. J. (2005). Mutant mice lacking acetyl-CoA carboxylase 1 are embryonically lethal. *Proceedings of the National Academy of Sciences*, *102*(34), 12011–12016. https://doi.org/10.1073/pnas.0505714102

Abu-Elheiga, L., Oh, W., Kordari, P., & Wakil, S. J. (2003). Acetyl-CoA carboxylase 2 mutant mice are protected against obesity and diabetes induced by high-fat/high-carbohydrate diets. *Proceedings of the National Academy of Sciences*, *100*(18), 10207–10212. https://doi.org/10.1073/pnas.1733877100

Andersen, J. V., Westi, E. W., Jakobsen, E., Urruticoechea, N., Borges, K., & Aldana, B. I. (2021). Astrocyte metabolism of the medium-chain fatty acids octanoic acid and decanoic acid promotes GABA synthesis in neurons via elevated glutamine supply. *Molecular Brain*, *14*(1), 132. https://doi.org/10.1186/s13041-021-00842-2

Asrih, M., Altirriba, J., Rohner-Jeanrenaud, F., & Jornayvaz, F. R. (2015). Ketogenic Diet Impairs FGF21 Signaling and Promotes Differential Inflammatory Responses in the Liver and White Adipose Tissue. *PLOS ONE*, *10*(5), e0126364. https://doi.org/10.1371/journal.pone.0126364

Augustin, K., Khabbush, A., Williams, S., Eaton, S., Orford, M., Cross, J. H., Heales, S. J. R., Walker, M. C., & Williams, R. S. B. (2018). Mechanisms of action for the medium-chain triglyceride ketogenic diet in neurological and metabolic disorders. *The Lancet Neurology*, *17*(1), 84–93. https://doi.org/10.1016/S1474-4422(17)30408-8

Austin, S., Mekis, R., Mohammed, S. E. M., Scalise, M., Wang, W., Galluccio, M., Pfeiffer, C., Borovec, T., Parapatics, K., Vitko, D., Dinhopl, N., Demaurex, N., Bennett, K. L., Indiveri, C., & Nowikovsky, K. (2022). TMBIM5 is the Ca2+/H+ antiporter of mammalian mitochondria. *EMBO reports*, *23*(12), e54978. https://doi.org/10.15252/embr.202254978

Bal, N. C., Singh, S., Reis, F. C. G., Maurya, S. K., Pani, S., Rowland, L. A., & Periasamy, M. (2017). Both brown adipose tissue and skeletal muscle thermogenesis processes are activated during mild to severe cold adaptation in mice. *Journal of Biological Chemistry*, *292*(40), 16616–16625. https://doi.org/10.1074/jbc.M117.790451

Beccaria, M., Sullini, G., Cacciola, F., Donato, P., Dugo, P., & Mondello, L. (2014). High performance characterization of triacylglycerols in milk and milk-related samples by liquid chromatography and mass spectrometry. *Journal of Chromatography A*, *1360*, 172–187. https://doi.org/10.1016/j.chroma.2014.07.073

Borowicz-Reutt, K., Krawczyk, M., & Czernia, J. (2024). Ketogenic Diet in the Treatment of Epilepsy. *Nutrients*, *16*(9), Article 9. https://doi.org/10.3390/nu16091258

Cannon, B., & Nedergaard, J. (2004). Brown Adipose Tissue: Function and Physiological Significance. *Physiological Reviews*, *84*(1), 277–359. https://doi.org/10.1152/physrev.00015.2003

Carpentier, A. C., Blondin, D. P., Virtanen, K. A., Richard, D., Haman, F., & Turcotte, É. E. (2018). Brown Adipose Tissue Energy Metabolism in Humans. *Frontiers in Endocrinology*, *9*, 447. https://doi.org/10.3389/fendo.2018.00447

Castle, J. C., Hara, Y., Raymond, C. K., Garrett-Engele, P., Ohwaki, K., Kan, Z., Kusunoki, J., & Johnson, J. M. (2009). ACC2 Is Expressed at High Levels Human White Adipose and Has an Isoform with a Novel N-Terminus. *PLoS ONE*, *4*(2), e4369. https://doi.org/10.1371/journal.pone.0004369

Cedikova, M., Kripnerová, M., Dvorakova, J., Pitule, P., Grundmanova, M., Babuska, V., Mullerova, D., & Kuncova, J. (2016). Mitochondria in White, Brown, and Beige Adipocytes. *Stem Cells International*, *2016*(1), 6067349. https://doi.org/10.1155/2016/6067349

Charlot, A., Morel, L., Bringolf, A., Georg, I., Charles, A.-L., Goupilleau, F., Geny, B., & Zoll, J. (2022). Octanoic Acid-Enrichment Diet Improves Endurance Capacity and Reprograms Mitochondrial Biogenesis in Skeletal Muscle of Mice. *Nutrients*, *14*(13), Article 13. https://doi.org/10.3390/nu14132721

Cheng, X., Jiang, C., Jin, J., Jin, Q., Akoh, C. C., Wei, W., & Wang, X. (2024). Medium- and Long-Chain Triacylglycerol: Preparation, Health Benefits, and Food Utilization. *Annual Review of Food Science and Technology*, *15*(Volume 15, 2024), 381–408. https://doi.org/10.1146/annurev-food-072023-034539

Choy, K. Y. C., & Louie, J. C. Y. (2023). The effects of the ketogenic diet for the management of type 2 diabetes mellitus: A systematic review and meta-analysis of recent studies. *Diabetes & Metabolic Syndrome: Clinical Research & Reviews*, *17*(12), 102905. https://doi.org/10.1016/j.dsx.2023.102905

Corsello, A., Trovato, C. M., Di Profio, E., Cardile, S., Campoy, C., Zuccotti, G., Verduci, E., & Diamanti, A. (2023). Ketogenic diet in children and adolescents: The effects on growth and nutritional status. *Pharmacological Research*, *191*, 106780. https://doi.org/10.1016/j.phrs.2023.106780

Dambrova, M., Makrecka-Kuka, M., Kuka, J., Vilskersts, R., Nordberg, D., Attwood, M. M., Smesny, S., Sen, Z. D., Guo, A. C., Oler, E., Tian, S., Zheng, J., Wishart, D. S., Liepinsh, E., & Schiöth, H. B. (2022). Acylcarnitines: Nomenclature, Biomarkers, Therapeutic Potential, Drug Targets, and Clinical Trials. *Pharmacological Reviews*, *74*(3), 506–551. https://doi.org/10.1124/pharmrev.121.000408

Devine, J., Monzel, A. S., Shire, D., Rosenberg, A. M., Junker, A., Cohen, A. A., & Picard, M. (2025). Brain–body mitochondrial distribution patterns lack coherence and point to tissue-specific regulatory mechanisms. *Life Metabolism*, *4*(3), loaf012. https://doi.org/10.1093/lifemeta/loaf012

Dunn, E., Zhang, B., Sahota, V. K., & Augustin, H. (2023). Potential benefits of medium chain fatty acids in aging and neurodegenerative disease. *Frontiers in Aging Neuroscience*, *15*. https://doi.org/10.3389/fnagi.2023.1230467

Dyńka, D., Kowalcze, K., Charuta, A., & Paziewska, A. (2023). The Ketogenic Diet and Cardiovascular Diseases. *Nutrients*, *15*(15), 3368. https://doi.org/10.3390/nu15153368

Fafián-Labora, J., Carpintero-Fernández, P., Jordan, S. J. D., Shikh-Bahaei, T., Abdullah, S. M., Mahenthiran, M., Rodríguez-Navarro, J. A., Niklison-Chirou, M. V., & O'Loghlen, A. (2019). FASN activity is important for the initial stages of the induction of senescence. *Cell Death & Disease*, *10*(4), 1–15. https://doi.org/10.1038/s41419-019-1550-0

Falkenhain, K., Daraei, A., Forbes, S. C., & Little, J. P. (2022). Effects of Exogenous Ketone Supplementation on Blood Glucose: A Systematic Review and Meta-analysis. *Advances in Nutrition*, *13*(5), 1697–1714. https://doi.org/10.1093/advances/nmac036

Farooqi, I. S., & Xu, Y. (2024). Translational potential of mouse models of human metabolic disease. *Cell*, *187*(16), 4129–4143. https://doi.org/10.1016/j.cell.2024.07.011

Ferraris, C., Guglielmetti, M., Pasca, L., De Giorgis, V., Ferraro, O. E., Brambilla, I., Leone, A., De Amicis, R., Bertoli, S., Veggiotti, P., & Tagliabue, A. (2019). Impact of the Ketogenic Diet on Linear Growth in Children: A Single-Center Retrospective Analysis of 34 Cases. *Nutrients*, *11*(7), 1442. https://doi.org/10.3390/nu11071442

Fortier, M., Castellano, C., St-Pierre, V., Myette-Côté, É., Langlois, F., Roy, M., Morin, M., Bocti, C., Fulop, T., Godin, J., Delannoy, C., Cuenoud, B., & Cunnane, S. C. (2021). A ketogenic drink improves cognition in mild cognitive impairment: Results of a 6-month RCT. *Alzheimer's & Dementia*, *17*(3), 543–552. https://doi.org/10.1002/alz.12206

Frontini, A., & Cinti, S. (2010). Distribution and Development of Brown Adipocytes in the Murine and Human Adipose Organ. *Cell Metabolism*, *11*(4), 253–256. https://doi.org/10.1016/j.cmet.2010.03.004

Fujikura, Y., Sugihara, H., Hatakeyama, M., Oishi, K., & Yamanouchi, K. (2021). Ketogenic diet with medium-chain triglycerides restores skeletal muscle function and pathology in a rat model of Duchenne muscular dystrophy. *The FASEB Journal*, *35*(9), e21861. https://doi.org/10.1096/fj.202100629R

Gallardo-Montejano, V. I., Saxena, G., Kusminski, C. M., Yang, C., McAfee, J. L., Hahner, L., Hoch, K., Dubinsky, W., Narkar, V. A., & Bickel, P. E. (2016).

Nuclear Perilipin 5 integrates lipid droplet lipolysis with PGC-1α/SIRT1-dependent transcriptional regulation of mitochondrial function. *Nature Communications*, *7*(1), 12723. https://doi.org/10.1038/ncomms12723

Goetzman, E. S., Bharathi, S. S., Zhang, Y., Zhao, X.-J., Dobrowolski, S. F., Peasley, K., Sims-Lucas, S., & Monga, S. P. (2020). Impaired mitochondrial medium-chain fatty acid oxidation drives periportal macrovesicular steatosis in sirtuin-5 knockout mice. *Scientific Reports*, *10*(1), 18367. https://doi.org/10.1038/s41598-020-75615-3

Gregor, A., Huber, L., Auernigg-Haselmaier, S., Sternberg, F., Billerhart, M., Dunkel, A., Somoza, V., Ogris, M., Kofler, B., Longo, V. D., König, J., & Duszka, K. (2022). A Comparison of the Impact of Restrictive Diets on the Gastrointestinal Tract of Mice. *Nutrients*, *14*(15), Article 15. https://doi.org/10.3390/nu14153120

Guo, Y., Wu, H., Wiesmüller, L., & Chen, M. (2024). Canonical and non-canonical functions of p53 isoforms: Potentiating the complexity of tumor development and therapy resistance. *Cell Death & Disease*, *15*(6), 1–16. https://doi.org/10.1038/s41419-024-06783-7

Hamsanathan, S., & Gurkar, A. U. (2022). Lipids as Regulators of Cellular Senescence. *Frontiers in Physiology*, *13*. https://doi.org/10.3389/fphys.2022.796850

Haslam, R. L., Bezzina, A., Herbert, J., Spratt, N., Rollo, M. E., & Collins, C. E. (2021). Can Ketogenic Diet Therapy Improve Migraine Frequency, Severity and Duration? *Healthcare*, *9*(9), 1105. https://doi.org/10.3390/healthcare9091105

He, Q., Au, B., Kulkarni, M., Shen, Y., Lim, Kah. J., Maimaiti, J., Wong, Cheng. Kit., Luijten, Monique. N. H., Chong, H. C., Lim, E. H., Rancati, G., Sinha, I., Fu, Z., Wang, X., Connolly, John. E., & Crasta, K. C. (2018). Chromosomal instability-induced senescence potentiates cell non-autonomous tumourigenic effects. *Oncogenesis*, *7*(8), 62. https://doi.org/10.1038/s41389-018-0072-4

Herbers, E., Kekäläinen, N. J., Hangas, A., Pohjoismäki, J. L., & Goffart, S. (2019). Tissue specific differences in mitochondrial DNA maintenance and expression. *Mitochondrion*, *44*, 85–92. https://doi.org/10.1016/j.mito.2018.01.004

Hernandez-Quiles, M., Broekema, M. F., & Kalkhoven, E. (2021). PPARgamma in Metabolism, Immunity, and Cancer: Unified and Diverse Mechanisms of Action. *Frontiers in Endocrinology*, *12*. https://doi.org/10.3389/fendo.2021.624112

Huang, L., Gao, L., & Chen, C. (2021). Role of Medium-Chain Fatty Acids in Healthy Metabolism: A Clinical Perspective. *Trends in Endocrinology & Metabolism*, *32*(6), 351–366. https://doi.org/10.1016/j.tem.2021.03.002

Hughes, S. D., Kanabus, M., Anderson, G., Hargreaves, I. P., Rutherford, T., Donnell, M. O., Cross, J. H., Rahman, S., Eaton, S., & Heales, S. J. R. (2014). The ketogenic diet component decanoic acid increases mitochondrial citrate synthase and complex I activity in neuronal cells. *Journal of Neurochemistry*, *129*(3), 426–433. https://doi.org/10.1111/jnc.12646

Ihenacho, U. K., Meacham, K. A., Harwig, M. C., Widlansky, M. E., & Hill, R. B. (2021). Mitochondrial Fission Protein 1: Emerging Roles in Organellar Form and Function in Health and Disease. *Frontiers in Endocrinology*, *12*, 660095. https://doi.org/10.3389/fendo.2021.660095

Ishizawa, R., Masuda, K., Sakata, S., & Nakatani, A. (2015). Effects of Different Fatty Acid Chain Lengths on Fatty Acid Oxidation-Related Protein Expression Levels in Rat Skeletal Muscles. *Journal of Oleo Science*, *64*(4), 415–421. https://doi.org/10.5650/jos.ess14199

Jang, J., Kim, S. R., Lee, J. E., Lee, S., Son, H. J., Choe, W., Yoon, K.-S., Kim, S. S., Yeo, E.-J., & Kang, I. (2023). Molecular Mechanisms of Neuroprotection by Ketone Bodies and Ketogenic Diet in Cerebral Ischemia and Neurodegenerative Diseases. *International Journal of Molecular Sciences*, *25*(1), 124. https://doi.org/10.3390/ijms25010124

Jensen, N. J., Wodschow, H. Z., Nilsson, M., & Rungby, J. (2020). Effects of Ketone Bodies on Brain Metabolism and Function in Neurodegenerative Diseases. *International Journal of Molecular Sciences*, *21*(22), 8767. https://doi.org/10.3390/ijms21228767

Joruiz, S., & Bourdon, J. (2016). p53 Isoforms: Key Regulators of the Cell Fate Decision. *Cold Spring Harbor Perspectives in Medicine*, *6*, a026039. https://doi.org/10.1101/cshperspect.a026039

Kanabus, M., Fassone, E., Hughes, S. D., Bilooei, S. F., Rutherford, T., Donnell, M. O., Heales, S. J. R., & Rahman, S. (2016). The pleiotropic effects of decanoic acid treatment on mitochondrial function in fibroblasts from patients with complex I deficient Leigh syndrome. *Journal of Inherited Metabolic Disease*, *39*(3), 415–426. https://doi.org/10.1007/s10545-016-9930-4

Karagöz, M. F., & Gülçin Sağdıçoğlu Celep, A. (2023). The effect of caloric restriction on genetical pathways. *Food Science and Human Wellness*, *12*(5), 1450–1457. https://doi.org/10.1016/j.fshw.2023.02.007

Khabbush, A., Orford, M., Tsai, Y.-C., Rutherford, T., O'Donnell, M., Eaton, S., & Heales, S. J. R. (2017). Neuronal decanoic acid oxidation is markedly lower than that of octanoic acid: A mechanistic insight into the medium-chain triglyceride ketogenic diet. *Epilepsia*, *58*(8), 1423–1429. https://doi.org/10.1111/epi.13833

Kim, Y. Y., Um, J., Yoon, J., Lee, D., Lee, Y. J., Kim, D. H., Park, J., & Yun, J. (2020). P53 regulates mitochondrial dynamics by inhibiting Drp1 translocation into mitochondria during cellular senescence. *The FASEB Journal*, *34*(2), 2451–2464. https://doi.org/10.1096/fj.201901747RR

Kleele, T., Rey, T., Winter, J., Zaganelli, S., Mahecic, D., Perreten Lambert, H., Ruberto, F. P., Nemir, M., Wai, T., Pedrazzini, T., & Manley, S. (2021). Distinct fission signatures predict mitochondrial degradation or biogenesis. *Nature*, *593*(7859), 435–439. https://doi.org/10.1038/s41586-021-03510-6

Kolb, H., Kempf, K., Röhling, M., Lenzen-Schulte, M., Schloot, N. C., & Martin, S. (2021). Ketone bodies: From enemy to friend and guardian angel. *BMC Medicine*, *19*(1), 313. https://doi.org/10.1186/s12916-021-02185-0

Kytikova, O. Yu., Perelman, J. M., Novgorodtseva, T. P., Denisenko, Y. K., Kolosov, V. P., Antonyuk, M. V., & Gvozdenko, T. A. (2020). Peroxisome Proliferator-Activated Receptors as a Therapeutic Target in Asthma. *PPAR Research*, *2020*(1), 8906968. https://doi.org/10.1155/2020/8906968

Lage, R., Diéguez, C., Vidal-Puig, A., & López, M. (2008). AMPK: A metabolic gauge regulating whole-body energy homeostasis. *Trends in Molecular Medicine*, *14*(12), 539–549. https://doi.org/10.1016/j.molmed.2008.09.007

Lee, S., Jeong, S.-Y., Lim, W.-C., Kim, S., Park, Y.-Y., Sun, X., Youle, R. J., & Cho, H. (2007). Mitochondrial Fission and Fusion Mediators, hFis1 and OPA1, Modulate Cellular Senescence. *Journal of Biological Chemistry*, *282*(31), 22977–22983. https://doi.org/10.1074/jbc.M700679200

Li, S., Zhuge, A., Wang, K., Lv, L., Bian, X., Yang, L., Xia, J., Jiang, X., Wu, W., Wang, S., Wang, Q., & Li, L. (2021). Ketogenic diet aggravates colitis, impairs intestinal barrier and alters gut microbiota and metabolism in DSS-induced mice. *Food & Function*, *12*(20), 10210–10225. https://doi.org/10.1039/D1FO02288A

Liberato, M. V., Nascimento, A. S., Ayers, S. D., Lin, J. Z., Cvoro, A., Silveira, R. L., Martínez, L., Souza, P. C. T., Saidemberg, D., Deng, T., Amato, A. A., Togashi, M., Hsueh, W. A., Phillips, K., Palma, M. S., Neves, F. A. R., Skaf, M. S., Webb, P., & Polikarpov, I. (2012). Medium Chain Fatty Acids Are Selective Peroxisome Proliferator Activated Receptor (PPAR) γ Activators and Pan-PPAR Partial Agonists. *PLOS ONE*, *7*(5), e36297. https://doi.org/10.1371/journal.pone.0036297

Liesa, M., & Shirihai, O. S. (2013). Mitochondrial Dynamics in the Regulation of Nutrient Utilization and Energy Expenditure. *Cell Metabolism*, *17*(4), 491–506. https://doi.org/10.1016/j.cmet.2013.03.002

Lin, T.-Y., Liu, H.-W., & Hung, T.-M. (2021). The Ketogenic Effect of Medium-Chain Triacylglycerides. *Frontiers in Nutrition*, *8*. https://doi.org/10.3389/fnut.2021.747284

Longo, V. D., Di Tano, M., Mattson, M. P., & Guidi, N. (2021). Intermittent and periodic fasting, longevity and disease. *Nature Aging*, *1*(1), 47–59. https://doi.org/10.1038/s43587-020-00013-3

Malapaka, R. R. V., Khoo, S., Zhang, J., Choi, J. H., Zhou, X. E., Xu, Y., Gong, Y., Li, J., Yong, E.-L., Chalmers, M. J., Chang, L., Resau, J. H., Griffin, P. R.,

Chen, Y. E., & Xu, H. E. (2012). Identification and Mechanism of 10-Carbon Fatty Acid as Modulating Ligand of Peroxisome Proliferator-activated Receptors *. *Journal of Biological Chemistry*, *287*(1), 183–195. https://doi.org/10.1074/jbc.M111.294785

Marlatt, K. L., Chen, K. Y., & Ravussin, E. (2018). Is activation of human brown adipose tissue a viable target for weight management? *American Journal of Physiology-Regulatory, Integrative and Comparative Physiology*, *315*(3), R479–R483. https://doi.org/10.1152/ajpregu.00443.2017

Martines, A.-C. M. F., Gerding, A., Stolle, S., Vieira-Lara, M. A., Wolters, J. C., Jurdzinski, A., Bongiovanni, L., De Bruin, A., Van Der Vlies, P., Van Der Vries, G., Bloks, V. W., Derks, T. G. J., Reijngoud, D.-J., & Bakker, B. M. (2019). Transcriptome analysis suggests a compensatory role of the cofactors coenzyme A and NAD+ in medium-chain acyl-CoA dehydrogenase knockout mice. *Scientific Reports*, *9*(1), 14539. https://doi.org/10.1038/s41598-019-50758-0

Mason, E., Hindmarch, C. C. T., & Dunham-Snary, K. J. (2023). Medium-chain Acyl-COA dehydrogenase deficiency: Pathogenesis, diagnosis, and treatment. *Endocrinology, Diabetes & Metabolism*, *6*(1), e385. https://doi.org/10.1002/edm2.385

Merlotti, D., Cosso, R., Eller-Vainicher, C., Vescini, F., Chiodini, I., Gennari, L., & Falchetti, A. (2021). Energy Metabolism and Ketogenic Diets: What about the Skeletal Health? A Narrative Review and a Prospective Vision for Planning Clinical Trials on this Issue. *International Journal of Molecular Sciences*, *22*(1), 435. https://doi.org/10.3390/ijms22010435

Miranda, M. J., Turner, Z., & Magrath, G. (2012). Alternative diets to the classical ketogenic diet—Can we be more liberal? *Epilepsy Research*, *100*(3), 278–285. https://doi.org/10.1016/j.eplepsyres.2012.06.007

Misko, A., Jiang, S., Wegorzewska, I., Milbrandt, J., & Baloh, R. H. (2010). Mitofusin 2 Is Necessary for Transport of Axonal Mitochondria and Interacts with the Miro/Milton Complex. *Journal of Neuroscience*, *30*(12), 4232–4240. https://doi.org/10.1523/JNEUROSCI.6248-09.2010

Møller, N. (2020). Ketone Body, 3-Hydroxybutyrate: Minor Metabolite - Major Medical Manifestations. *The Journal of Clinical Endocrinology & Metabolism*, *105*(9), 2884–2892. https://doi.org/10.1210/clinem/dgaa370

Nelson, A. B., Queathem, E. D., Puchalska, P., & Crawford, P. A. (2023). Metabolic Messengers: Ketone bodies. *Nature Metabolism*, *5*(12), 2062–2074. https://doi.org/10.1038/s42255-023-00935-3

Ngo, J., Choi, D. W., Stanley, I. A., Stiles, L., Molina, A. J. A., Chen, P., Lako, A., Sung, I. C. H., Goswami, R., Kim, M., Miller, N., Baghdasarian, S., Kim-Vasquez, D., Jones, A. E., Roach, B., Gutierrez, V., Erion, K., Divakaruni, A. S., Liesa, M., … Shirihai, O. S. (2023). Mitochondrial morphology controls fatty acid utilization by changing CPT1 sensitivity to malonyl-CoA. *The*

EMBO Journal, *42*(11), e111901. https://doi.org/10.15252/embj.2022111901

Nicastro, R., Brohée, L., Alba, J., Nüchel, J., Figlia, G., Kipschull, S., Gollwitzer, P., Romero-Pozuelo, J., Fernandes, S. A., Lamprakis, A., Vanni, S., Teleman, A. A., De Virgilio, C., & Demetriades, C. (2023). Malonyl-CoA is a conserved endogenous ATP-competitive mTORC1 inhibitor. *Nature Cell Biology*, *25*(9), 1303–1318. https://doi.org/10.1038/s41556-023-01198-6

Nimbkar, S., Leena, M. M., Moses, J. A., & Anandharamakrishnan, C. (2022). Medium chain triglycerides (MCT): State-of-the-art on chemistry, synthesis, health benefits and applications in food industry. *Comprehensive Reviews in Food Science and Food Safety*, *21*(2), 843–867. https://doi.org/10.1111/1541-4337.12926

Nishida, R., Nukaga, S., Kawahara, I., Miyagawa, Y., Goto, K., Nakashima, C., Luo, Y., Sasaki, T., Fujii, K., Ohmori, H., Ogata, R., Mori, S., Fujiwara-Tani, R., & Kuniyasu, H. (2024). Differential Effects of Three Medium-Chain Fatty Acids on Mitochondrial Quality Control and Skeletal Muscle Maturation. *Antioxidants*, *13*(7), Article 7. https://doi.org/10.3390/antiox13070821

Noone, J., O'Gorman, D. J., & Kenny, H. C. (2022). OPA1 regulation of mitochondrial dynamics in skeletal and cardiac muscle. *Trends in Endocrinology & Metabolism*, *33*(10), 710–721. https://doi.org/10.1016/j.tem.2022.07.003

Norgren, J., Sindi, S., Sandebring-Matton, A., Kåreholt, I., Daniilidou, M., Akenine, U., Nordin, K., Rosenborg, S., Ngandu, T., & Kivipelto, M. (2020). Ketosis After Intake of Coconut Oil and Caprylic Acid—With and Without Glucose: A Cross-Over Study in Healthy Older Adults. *Frontiers in Nutrition*, *7*, 40. https://doi.org/10.3389/fnut.2020.00040

O'Leary, N. A., Wright, M. W., Brister, J. R., Ciufo, S., Haddad, D., McVeigh, R., Rajput, B., Robbertse, B., Smith-White, B., Ako-Adjei, D., Astashyn, A., Badretdin, A., Bao, Y., Blinkova, O., Brover, V., Chetvernin, V., Choi, J., Cox, E., Ermolaeva, O., … Pruitt, K. D. (2016). Reference sequence (RefSeq) database at NCBI: Current status, taxonomic expansion, and functional annotation. *Nucleic Acids Research*, *44*(D1), D733–D745. https://doi.org/10.1093/nar/gkv1189

Öztürk, E., Aslan Çin, N. N., Cansu, A., & Akyol, A. (2024). Ketogenic diet as a therapeutic approach in autism spectrum disorder: A narrative review. *Metabolic Brain Disease*, *40*(1), 67. https://doi.org/10.1007/s11011-024-01506-5

Pani, S., Dey, S., Pati, B., Senapati, U., & Bal, N. C. (2022). Brown to White Fat Transition Overlap With Skeletal Muscle During Development of Larger Mammals: Is it a Coincidence? *Journal of the Endocrine Society*, *6*(12), bvac151. https://doi.org/10.1210/jendso/bvac151

Pap, A., Cuaranta-Monroy, I., Peloquin, M., & Nagy, L. (2016). Is the Mouse a Good Model of Human PPARγ-Related Metabolic Diseases? *International*

Journal of Molecular Sciences, *17*(8), 1236. https://doi.org/10.3390/ijms17081236

Pereyra, A. S., McLaughlin, K. L., Buddo, K. A., & Ellis, J. M. (2023). Medium-chain fatty acid oxidation is independent of L -carnitine in liver and kidney but not in heart and skeletal muscle. *American Journal of Physiology-Gastrointestinal and Liver Physiology*, *325*(4), G287–G294. https://doi.org/10.1152/ajpgi.00105.2023

Pietrzak, D., Kasperek, K., Rękawek, P., & Piątkowska-Chmiel, I. (2022). The Therapeutic Role of Ketogenic Diet in Neurological Disorders. *Nutrients*, *14*(9), 1952. https://doi.org/10.3390/nu14091952

Popiolek-Kalisz, J. (2024). Ketogenic diet and cardiovascular risk – state of the art review. *Current Problems in Cardiology*, *49*(3), 102402. https://doi.org/10.1016/j.cpcardiol.2024.102402

Popov, L. (2020). Mitochondrial biogenesis: An update. *Journal of Cellular and Molecular Medicine*, *24*(9), 4892–4899. https://doi.org/10.1111/jcmm.15194

Porter, C., Herndon, D. N., Chondronikola, M., Chao, T., Annamalai, P., Bhattarai, N., Saraf, M. K., Capek, K. D., Reidy, P. T., Daquinag, A. C., Kolonin, M. G., Rasmussen, B. B., Borsheim, E., Toliver-Kinsky, T., & Sidossis, L. S. (2016). Human and Mouse Brown Adipose Tissue Mitochondria Have Comparable UCP1 Function. *Cell Metabolism*, *24*(2), 246–255. https://doi.org/10.1016/j.cmet.2016.07.004

Puchalska, P., & Crawford, P. A. (2017). Multi-dimensional Roles of Ketone Bodies in Fuel Metabolism, Signaling, and Therapeutics. *Cell Metabolism*, *25*(2), 262–284. https://doi.org/10.1016/j.cmet.2016.12.022

Pustjens, A. M., Boerrigter-Eenling, R., Koot, A. H., Rozijn, M., & Van Ruth, S. M. (2017). Characterization of Retail Conventional, Organic, and Grass Full-Fat Butters by Their Fat Contents, Free Fatty Acid Contents, and Triglyceride and Fatty Acid Profiling. *Foods*, *6*(4), Article 4. https://doi.org/10.3390/foods6040026

Rittner, A., Paithankar, K. S., Himmler, A., & Grininger, M. (2020). Type I fatty acid synthase trapped in the octanoyl-bound state. *Protein Science : A Publication of the Protein Society*, *29*(2), 589. https://doi.org/10.1002/pro.3797

Roehl, K., & Sewak, S. L. (2017). Practice Paper of the Academy of Nutrition and Dietetics: Classic and Modified Ketogenic Diets for Treatment of Epilepsy. *Journal of the Academy of Nutrition and Dietetics*, *117*(8), 1279–1292. https://doi.org/10.1016/j.jand.2017.06.006

Rydell-Törmänen, K., & Johnson, J. R. (2019). The Applicability of Mouse Models to the Study of Human Disease. In *Mouse Cell Culture* (S. 3–22). Humana Press, New York, NY. https://doi.org/10.1007/978-1-4939-9086-3_1

Saito, M. (2013). Brown adipose tissue as a therapeutic target for human obesity. *Obesity Research & Clinical Practice*, *7*(6), e432–e438. https://doi.org/10.1016/j.orcp.2013.09.001

Schönfeld, P., & Wojtczak, L. (2016). Short- and medium-chain fatty acids in energy metabolism: The cellular perspective. *Journal of Lipid Research*, *57*(6), 943–954. https://doi.org/10.1194/jlr.R067629

Seki, T., Yang, Y., Sun, X., Lim, S., Xie, S., Guo, Z., Xiong, W., Kuroda, M., Sakaue, H., Hosaka, K., Jing, X., Yoshihara, M., Qu, L., Li, X., Chen, Y., & Cao, Y. (2022). Brown-fat-mediated tumour suppression by cold-altered global metabolism. *Nature*, *608*(7922), 421–428. https://doi.org/10.1038/s41586-022-05030-3

Shcherbakova, K., Schwarz, A., Apryatin, S., Karpenko, M., & Trofimov, A. (2022). Supplementation of Regular Diet With Medium-Chain Triglycerides for Pro-cognitive Effects: A Narrative Review. *Frontiers in Nutrition*, *9*, 934497. https://doi.org/10.3389/fnut.2022.934497

Sidarala, V., Zhu, J., Levi-D'Ancona, E., Pearson, G. L., Reck, E. C., Walker, E. M., Kaufman, B. A., & Soleimanpour, S. A. (2022). Mitofusin 1 and 2 regulation of mitochondrial DNA content is a critical determinant of glucose homeostasis. *Nature Communications*, *13*(1), 2340. https://doi.org/10.1038/s41467-022-29945-7

Song, M. J., Park, C., Kim, H., Han, S., Lee, S. H., Lee, D. H., & Chung, J. H. (2023). Carnitine acetyltransferase deficiency mediates mitochondrial dysfunction-induced cellular senescence in dermal fibroblasts. *Aging Cell*, *22*(11), e14000. https://doi.org/10.1111/acel.14000

Speakman, J. R., & Keijer, J. (2012). Not so hot: Optimal housing temperatures for mice to mimic the thermal environment of humans. *Molecular Metabolism*, *2*(1), 5–9. https://doi.org/10.1016/j.molmet.2012.10.002

Sternberg, F., Sternberg, C., Dunkel, A., Beikbaghban, T., Gregor, A., Szarzynski, A., Somoza, V., Walter, I., Duszka, K., Kofler, B., & Pohl, E. E. (2023). Ketogenic diets composed of long-chain and medium-chain fatty acids induce cardiac fibrosis in mice. *Molecular Metabolism*, *72*, 101711. https://doi.org/10.1016/j.molmet.2023.101711

St-Pierre, V., Vandenberghe, C., Lowry, C.-M., Fortier, M., Castellano, C.-A., Wagner, R., & Cunnane, S. C. (2019). Plasma Ketone and Medium Chain Fatty Acid Response in Humans Consuming Different Medium Chain Triglycerides During a Metabolic Study Day. *Frontiers in Nutrition*, *6*. https://doi.org/10.3389/fnut.2019.00046

Stride, N., Larsen, S., Treebak, J. T., Hansen, C. N., Hey-Mogensen, M., Speerschneider, T., Jensen, T. E., Jeppesen, J., Wojtaszewski, J. F. P., Richter, E. A., Køber, L., & Dela, F. (2012). 5′-AMP Activated Protein Kinase is Involved in the Regulation of Myocardial β-Oxidative Capacity in Mice. *Frontiers in Physiology*, *3*. https://doi.org/10.3389/fphys.2012.00033

Sun, Y., Zhou, D., Wang, Y., Wang, Z., Zhang, D., Qian, Z., Yan, J., Li, Z., Huang, G., & Li, W. (2024). Medium-chain triglycerides combined with DHA improve cognitive function by inhibiting neurocyte apoptosis of the brain in SAMP8 mice. *Experimental Gerontology*, *194*, 112520. https://doi.org/10.1016/j.exger.2024.112520

Tábara, L.-C., Segawa, M., & Prudent, J. (2024). Molecular mechanisms of mitochondrial dynamics. *Nature Reviews Molecular Cell Biology*, 1–24. https://doi.org/10.1038/s41580-024-00785-1

Talib, W. H., Mahmod, A. I., Kamal, A., Rashid, H. M., Alashqar, A. M. D., Khater, S., Jamal, D., & Waly, M. (2021). Ketogenic Diet in Cancer Prevention and Therapy: Molecular Targets and Therapeutic Opportunities. *Current Issues in Molecular Biology*, *43*(2), 558–589. https://doi.org/10.3390/cimb43020042

Temaj, G., Chichiarelli, S., Telkoparan-Akillilar, P., Saha, S., Nuhii, N., Hadziselimovic, R., & Saso, L. (2024). P53: A key player in diverse cellular processes including nuclear stress and ribosome biogenesis, highlighting potential therapeutic compounds. *Biochemical Pharmacology*, *226*, 116332. https://doi.org/10.1016/j.bcp.2024.116332

The Alliance of Genome Resources Consortium. (2024). Updates to the Alliance of Genome Resources central infrastructure. *Genetics*, *227*(1), iyae049. https://doi.org/10.1093/genetics/iyae049

Timmons, J. A., Wennmalm, K., Larsson, O., Walden, T. B., Lassmann, T., Petrovic, N., Hamilton, D. L., Gimeno, R. E., Wahlestedt, C., Baar, K., Nedergaard, J., & Cannon, B. (2007). Myogenic gene expression signature establishes that brown and white adipocytes originate from distinct cell lineages. *Proceedings of the National Academy of Sciences*, *104*(11), 4401–4406. https://doi.org/10.1073/pnas.0610615104

Tong, L. (2005). Acetyl-coenzyme A carboxylase: Crucial metabolic enzyme and attractive target for drug discovery. *Cellular and Molecular Life Sciences CMLS*, *62*(16), 1784–1803. https://doi.org/10.1007/s00018-005-5121-4

Twig, G., Elorza, A., Molina, A. J. A., Mohamed, H., Wikstrom, J. D., Walzer, G., Stiles, L., Haigh, S. E., Katz, S., Las, G., Alroy, J., Wu, M., Py, B. F., Yuan, J., Deeney, J. T., Corkey, B. E., & Shirihai, O. S. (2008). Fission and selective fusion govern mitochondrial segregation and elimination by autophagy. *The EMBO Journal*, *27*(2), 433–446. https://doi.org/10.1038/sj.emboj.7601963

Volpicella, M., Sgobba, M. N., Laera, L., Francavilla, A. L., De Luca, D. I., Guerra, L., Pierri, C. L., & De Grassi, A. (2025). Carnitine O-Acetyltransferase as a Central Player in Lipid and Branched-Chain Amino Acid Metabolism, Epigenetics, Cell Plasticity, and Organelle Function. *Biomolecules*, *15*(2), Article 2. https://doi.org/10.3390/biom15020216

Vosselman, M. J., Hoeks, J., Brans, B., Pallubinsky, H., Nascimento, E. B. M., van der Lans, A. a. J. J., Broeders, E. P. M., Mottaghy, F. M., Schrauwen, P., & van Marken Lichtenbelt, W. D. (2015). Low brown adipose tissue activity in endurance-trained compared with lean sedentary men. *International Journal of Obesity*, *39*(12), 1696–1702. https://doi.org/10.1038/ijo.2015.130

Wai, T., & Langer, T. (2016). Mitochondrial Dynamics and Metabolic Regulation. *Trends in Endocrinology & Metabolism*, *27*(2), 105–117. https://doi.org/10.1016/j.tem.2015.12.001

Wallace, M. A., Aguirre, N. W., Marcotte, G. R., Marshall, A. G., Baehr, L. M., Hughes, D. C., Hamilton, K. L., Roberts, M. N., Lopez-Dominguez, J. A., Miller, B. F., Ramsey, J. J., & Baar, K. (2021). The ketogenic diet preserves skeletal muscle with aging in mice. *Aging Cell*, *20*(4), e13322. https://doi.org/10.1111/acel.13322

Wang, Y., Liu, Z., Han, Y., Xu, J., Huang, W., & Li, Z. (2018). Medium Chain Triglycerides enhances exercise endurance through the increased mitochondrial biogenesis and metabolism. *PLoS ONE*, *13*(2), e0191182. https://doi.org/10.1371/journal.pone.0191182

Wang, Y., Yu, W., Li, S., Guo, D., He, J., & Wang, Y. (2022). Acetyl-CoA Carboxylases and Diseases. *Frontiers in Oncology*, *12*. https://doi.org/10.3389/fonc.2022.836058

Watt, M. J., & Hoy, A. J. (2012). Lipid metabolism in skeletal muscle: Generation of adaptive and maladaptive intracellular signals for cellular function. *American Journal of Physiology-Endocrinology and Metabolism*, *302*(11), E1315–E1328. https://doi.org/10.1152/ajpendo.00561.2011

Wei, S.-J., Schell, J. R., Chocron, E. S., Varmazyad, M., Xu, G., Chen, W. H., Martinez, G. M., Dong, F. F., Sreenivas, P., Rolando Trevino, J., Jiang, H., Du, Y., Saliba, A., Qian, W., Lorenzana, B., Nazarullah, A., Chang, J., Sharma, K., Munkácsy, E., … Gius, D. (2024). Ketogenic diet induces p53-dependent cellular senescence in multiple organs. *Science Advances*, *10*(20), eado1463. https://doi.org/10.1126/sciadv.ado1463

Wei, W., Sun, C., Jiang, W., Zhang, X., Hong, Y., Jin, Q., Tao, G., Wang, X., & Yang, Z. (2019). Triacylglycerols fingerprint of edible vegetable oils by ultra-performance liquid chromatography-Q-ToF-MS. *LWT*, *112*, 108261. https://doi.org/10.1016/j.lwt.2019.108261

Wheless, J. W. (2008). History of the ketogenic diet. *Epilepsia*, *49*(s8), 3–5. https://doi.org/10.1111/j.1528-1167.2008.01821.x

Wlaź, P., Socała, K., Nieoczym, D., Żarnowski, T., Żarnowska, I., Czuczwar, S. J., & Gasior, M. (2015). Acute anticonvulsant effects of capric acid in seizure tests in mice. *Progress in Neuro-Psychopharmacology and Biological Psychiatry*, *57*, 110–116. https://doi.org/10.1016/j.pnpbp.2014.10.013

Włodarek, D. (2019). Role of Ketogenic Diets in Neurodegenerative Diseases (Alzheimer's Disease and Parkinson's Disease). *Nutrients*, *11*(1), 169. https://doi.org/10.3390/nu11010169

Wolf, D., Harris, N., Goldfinger, N., & Rotter, V. (1985). Isolation of a Full-Length Mouse cDNA Clone Coding for an Immunologically Distinct p53 Molecule. *Molecular and Cellular Biology*, *5*(1), 127–132. https://doi.org/10.1128/mcb.5.1.127-132.1985

Xu, S., Tao, H., Cao, W., Cao, L., Lin, Y., Zhao, S.-M., Xu, W., Cao, J., & Zhao, J.-Y. (2021). Ketogenic diets inhibit mitochondrial biogenesis and induce cardiac fibrosis. *Signal Transduction and Targeted Therapy*, *6*(1), 54. https://doi.org/10.1038/s41392-020-00411-4

Yahagi, N., Shimano, H., Matsuzaka, T., Najima, Y., Sekiya, M., Nakagawa, Y., Ide, T., Tomita, S., Okazaki, H., Tamura, Y., Iizuka, Y., Ohashi, K., Gotoda, T., Nagai, R., Kimura, S., Ishibashi, S., Osuga, J., & Yamada, N. (2003). P53 Activation in Adipocytes of Obese Mice*. *Journal of Biological Chemistry*, *278*(28), 25395–25400. https://doi.org/10.1074/jbc.M302364200

Yamasaki, M., Hasegawa, S., Ozaki, S., Imai, M., Saito, D., & Takahashi, N. (2023). High-Fat-Diet Suppressed Ketone Body Utilization for Lipogenic Pathway in Brown Adipose Tissues. *Metabolites*, *13*(4), 519. https://doi.org/10.3390/metabo13040519

Ye, J., Coulouris, G., Zaretskaya, I., Cutcutache, I., Rozen, S., & Madden, T. L. (2012). Primer-BLAST: A tool to design target-specific primers for polymerase chain reaction. *BMC Bioinformatics*, *13*, 134. https://doi.org/10.1186/1471-2105-13-134

Yue, F., Cheng, Y., Breschi, A., Vierstra, J., Wu, W., Ryba, T., Sandstrom, R., Ma, Z., Davis, C., Pope, B. D., Shen, Y., Pervouchine, D. D., Djebali, S., Thurman, R. E., Kaul, R., Rynes, E., Kirilusha, A., Marinov, G. K., Williams, B. A., … Ren, B. (2014). A comparative encyclopedia of DNA elements in the mouse genome. *Nature*, *515*(7527), 355–364. https://doi.org/10.1038/nature13992

Zanfardino, P., Amati, A., Perrone, M., & Petruzzella, V. (2025). The Balance of MFN2 and OPA1 in Mitochondrial Dynamics, Cellular Homeostasis, and Disease. *Biomolecules*, *15*(3), 433. https://doi.org/10.3390/biom15030433

Zhang, X., Xu, W., Xu, R., Wang, Z., Zhang, X., Wang, P., Peng, K., Li, M., Li, J., Tan, Y., Wang, X., & Pei, H. (2022). Plin5 Bidirectionally Regulates Lipid Metabolism in Oxidative Tissues. *Oxidative Medicine and Cellular Longevity*, *2022*(1), 4594956. https://doi.org/10.1155/2022/4594956

Zhang, Z., Sliter, D. A., Bleck, C. K. E., & Ding, S. (2019). Fis1 deficiencies differentially affect mitochondrial quality in skeletal muscle. *Mitochondrion*, *49*, 217–226. https://doi.org/10.1016/j.mito.2019.09.005

Zhou, C., Wang, M., Liang, J., He, G., & Chen, N. (2022). Ketogenic Diet Benefits to Weight Loss, Glycemic Control, and Lipid Profiles in Overweight Patients with Type 2 Diabetes Mellitus: A Meta-Analysis of Randomized Controlled Trails. *International Journal of Environmental Research and Public Health*, *19*(16), 10429. https://doi.org/10.3390/ijerph191610429

Zumbaugh, M. D., Johnson, S. E., Shi, T. H., & Gerrard, D. E. (2022). Molecular and biochemical regulation of skeletal muscle metabolism. *Journal of Animal Science*, *100*(8), skac035. https://doi.org/10.1093/jas/skac035

17. Lists of tables and figures

17.1 Tables

17.2 Figures

18. Supplementary data

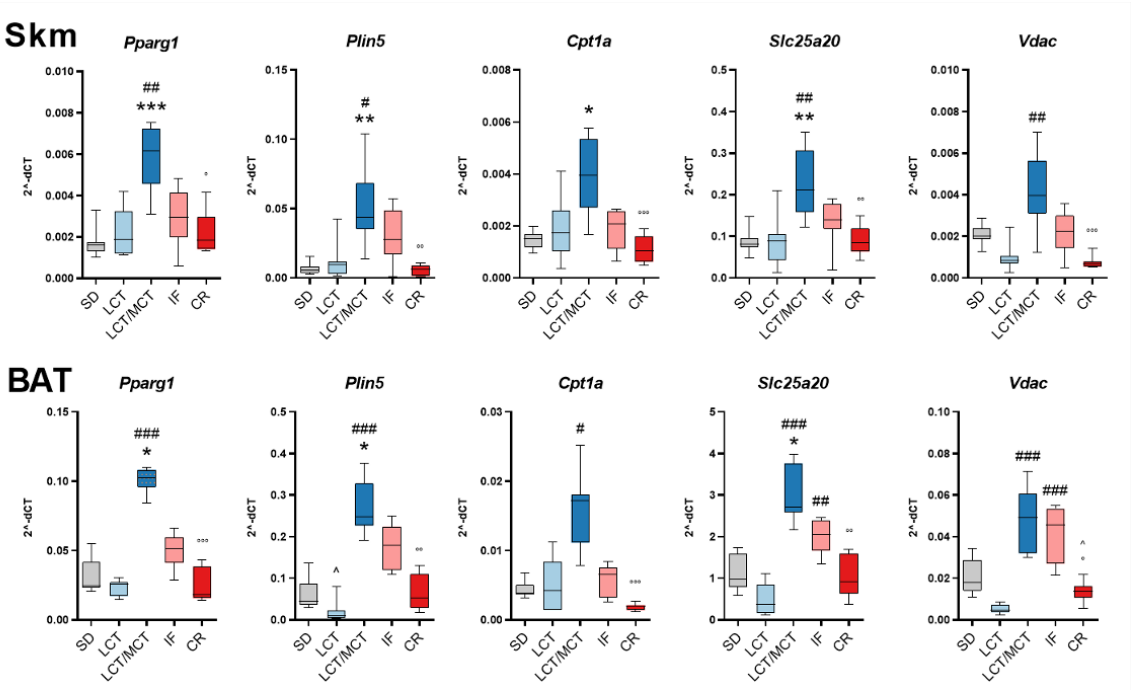

*Supplementary Figure 1: Relative mRNA levels of peroxisome proliferator activated receptor gamma 1 (Pparg1), perilipin 5 (Plin5), carnitine O-palmitoyltransferase 1a (Cpt1a), solute carrier family 25 (mitochondrial carnitine/acylcarnitine translocase), member 20 (Slc25a20) and voltage-dependent anion channel (Vdac) in skeletal muscle tissue (SkM) and brown adipose tissue (BAT) of mice fed SD, LCT, LCT/MCT, IF, CR diets after eight weeks. *P < 0.05, **P < 0.01, ***P < 0.001 vs. SD, # vs. LCT, o vs. LCT/MCT, ^ vs. IF. Statistical significance was assessed using nonparametric Kruskal-Wallis test, n = 6-8 individual mice/group. Standard diet (SD), Long-chain triglycerides (LCT), medium-chain triglycerides (MCT), Intermittent fasting (IF), Caloric restriction (CR), analyzed by Sternberg et al. (2025, unpublished data).*

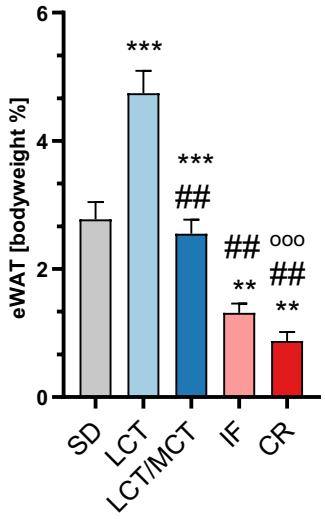

Supplementary Figure 2: % eWAT [to bodyweight], analyzed by Sternberg et al. (2025, unpublished data).

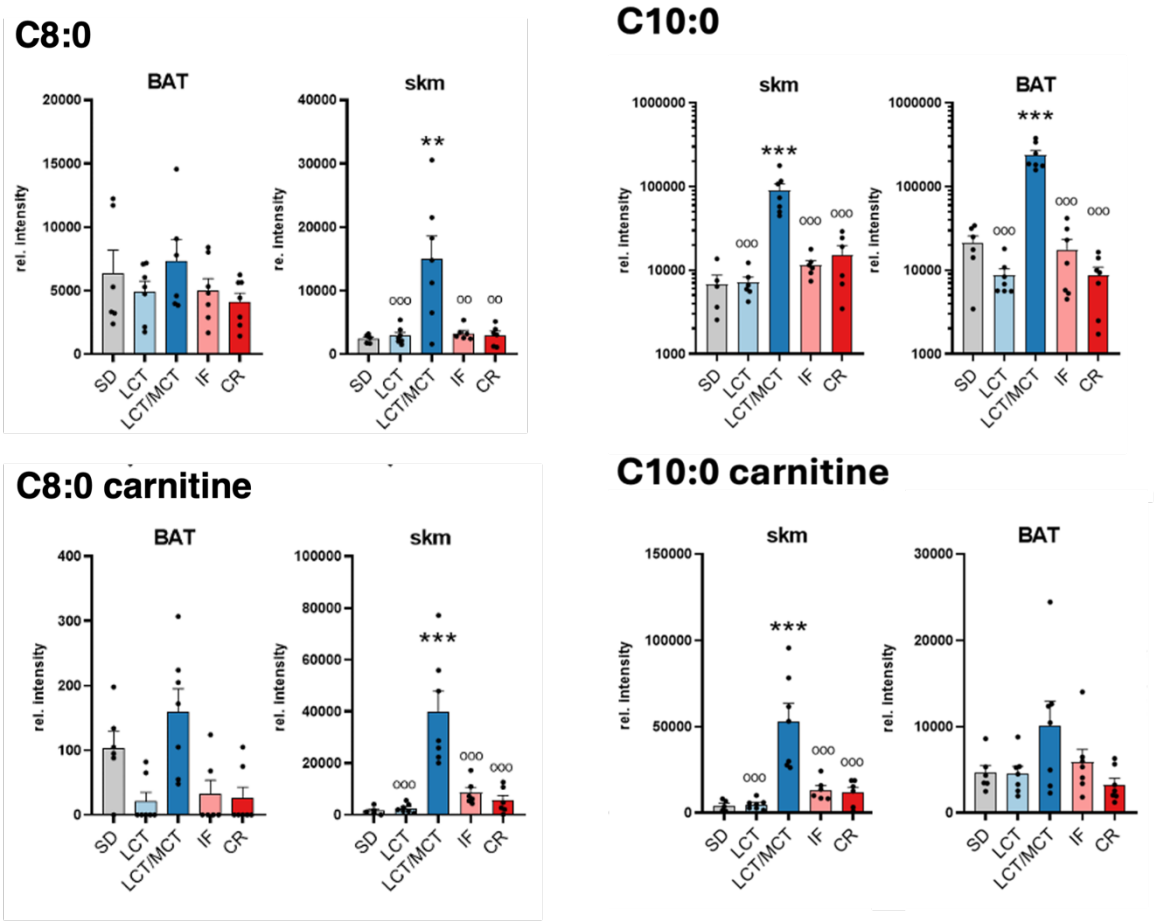

*Supplementary Figure 3: relative intensity of C8:0, C8:0 carnitine, C10:0 and C10:0 carnitine in BAT and SkM in SD, LCT, LCT/MCT, IF and CR, *P < 0.05, **P < 0.01, ***P < 0.001 vs. SD, # vs. LCT, o vs. LCT/MCT, ^ vs. IF, One-way ANOVA, analyzed by Sternberg et al. (2025, unpublished data).*

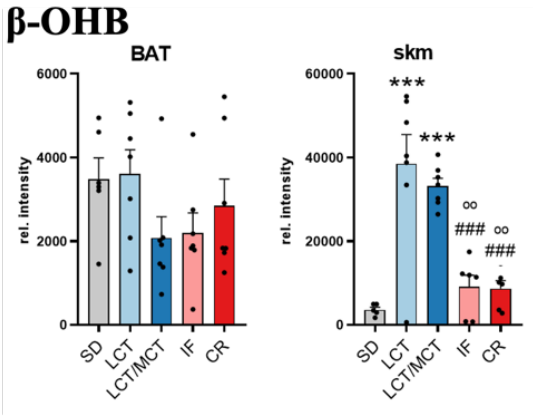

*Supplementary Figure 4: relative intensity of β-OHB in BAT and SkM in SD, LCT, LCT/MCT, IF and CR, *P < 0.05, **P < 0.01, ***P < 0.001 vs. SD, # vs. LCT, o vs. LCT/MCT, ^ vs. IF, One-way ANOVA, analyzed by Sternberg et al. (2025, unpublished data).*